Kinetics of Initiation, Propagation, and Termination for the [*rac*-(C_2H_4(1-indenyl)$_2$)ZrMe][MeB(C_6F_5)$_3$]-Catalyzed Polymerization of 1-Hexene

Zhixian Liu, Ekasith Somsook, Curtis B. White, Kimberly A. Rosaaen, and Clark R. Landis*

Contribution from the Department of Chemistry, University of Wisconsin—Madison, 1101 University Avenue, Madison, Wisconsin 53706

Received April 24, 2001

Abstract: Metallocene-catalyzed polymerization of 1-alkenes offers fine control of critical polymer attributes such as molecular weight, polydispersity, tacticity, and comonomer incorporation. Enormous effort has been expended on the synthesis and discovery of new catalysts and activators, but elementary aspects of the catalytic processes remain unclear. For example, it is unclear how the catalyst is distributed among active and dormant sites and how this distribution influences the order in monomer for the propagation rates, for which widely varying values are reported. Similarly, although empirical relationships between average molecular weights and monomer have been established for many systems, the underlying mechanisms of chain termination are unclear. Another area of intense interest concerns the role of ion-pairing in controlling the activity and termination mechanisms of metallocene-catalyzed polymerizations. Herein we report the application of quenched-flow kinetics, active site counting, polymer microstructure analysis, and molecular weight distribution analysis to the determination of fundamental rate laws for initiation, propagation, and termination for the polymerization of 1-hexene in toluene solution as catalyzed by the contact ion-pair, [*rac*-(C_2H_4(1-indenyl)$_2$)ZrMe][MeB(C_6F_5)$_3$] (**1**) over the temperature range of −10 to 50 °C. Highly isotactic (>99% *mmmm*) poly-1-hexene is produced with no apparent enchained regioerrors. Initiation and propagation processes are first order in the concentrations of 1-hexene and **1** but independent of excess borane or the addition of the contact ion-pair [$PhNMe_3$][MeB(C_6F_5)$_3$]. Active site counting and the reaction kinetics provide no evidence of catalyst accumulation in dormant or inactive sites. Initiation is slower than propagation by a factor of 70. The principal termination process is the formation of unsaturates of two types: vinylidene end groups that arise from termination after a 1,2 insertion and vinylene end groups that follow 2,1 insertions. The rate law for the former termination process is independent of the 1-hexene concentration, whereas the latter is first order. Analysis of ^{13}C-labeled polymer provides support for a mechanism of vinylene end group formation that is not chain transfer to monomer. Deterministic modeling of the molecular weight distributions using the fundamental rate laws and kinetic constants demonstrates the robustness of the kinetic analysis. Comparisons of insertion frequencies with estimated limits on the rates of ion-pair symmetrization obtained by NMR suggest that ion-pair separation prior to insertion is not required, but the analysis requires assumptions that cannot be validated.

Introduction

The advent of "single-site" metallocene catalysts for alkene polymerization has revolutionized industrial polyalkene synthesis.[1] With state-of-the-art metallocene catalysts it is possible to transform simple alkenes into polymers with rate accelerations and stereo- and regiospecificities that rival those of enzymic catalysts.[2] Catalysis is purely a kinetic phenomenon. Given the pervasive impact of metallocene catalysts on polyalkene production and research, it is surprising that there are no well-defined rate laws for the fundamental processes of initiation, propagation, and termination for a metallocene-catalyzed polymerization reaction with useful activity. In part, the lack of well-defined rate laws reflects difficulties posed by the high catalytic activities and the extreme sensitivity to impurities of metallocene catalysts. More restrictive is the problem of determining the fraction of metallocenes that are actively producing polymer in any instant, i.e., the active site count.[3] Without knowledge of the concentration and speciation of catalytically active species, it is impossible to correlate empirical rate laws with molecular mechanisms. Cocatalysts such as methylalumoxanes (MAO),[4] which comprise

(1) *Metallocene-Catalyzed Polymers: Materials, Properties, Processing and Markets*; Benedikt, G. M., Goodall, B. L., Eds.; Plastics Design Library: New York, 1998.

(2) For recent reviews relevant to this work, see: (a) Resconi, L.; Cavallo, L.; Fait, A.; Piemontesi, F. *Chem Rev.* **2000**, *100*, 1253−1345. (b) Chen, E. Y.-X.; Marks, T. J. *Chem. Rev.* **2000**, *100*, 1391−1434. (c) Alt, H. G.; Köppl, A. *Chem. Rev.* **2000**, *100*, 1205−1221. (d) Rappé, A. K.; Skiff, W. M.; Casewit, C. J. *Chem. Rev.* **2000**, *100*, 1435−1456. (e) Mashima, K.; Nakayama, Y.; Nakamura, A. *Adv. Polym. Sci.* **1997**, *133*, 1−51. (f) Hlatky, G. G. *Coord. Chem. Rev.* **1999**, *181*, 243−296. (g) Brintzinger, H.-H.; Fischer, D.; Miilhaupt, R.; Rieger, B.; Waymouth, R. M. *Angew. Chem., Int. Ed. Engl.* **1995**, *34*, 1143−1170.

(3) (a) Liu, Z.; Somsook, E.; Landis, C. R. *J. Am. Chem. Soc.* **2001**, *123*, 2915−2916. (b) Busico, V.; Cipullo, R.; Esposito, V. *Macromol. Rapid Commun.* **1999**, *20*, 116−121. (c) Marques, M. M.; Tait, P. J.; Mejzlik, J.; Dias, A. R. *J. Polym. Sci.: Part A, Polym. Chem.* **1998**, *36*, 573−585. (d) Han, T. K.; Ko, Y. S.; Park, J. W.; Woo, S. I. *Macromolecules* **1996**, *29*, 7305−7309. (e) Chien, J. C. W.; Tsai, W.-M. *Makromol. Chem., Macromol. Symp.* **1993**, *66*, 141−156. (f) Natta, G. *J. Polym. Sci.* **1959**, *34*, 21−48. (g) Chien, J. C. W.; Sugimoto, R. *J. Polym. Sci.: Part A, Polym. Chem.* **1991**, *29*, 459−470 (h) Busico, V.; Guardasole, M.; Margonelli, A.; Segre, A. L. *J. Am. Chem. Soc.* **2000**, *122*, 5226−5227.

10.1021/ja016072n CCC: $20.00
Published on Web 10/17/2001

Scheme 1

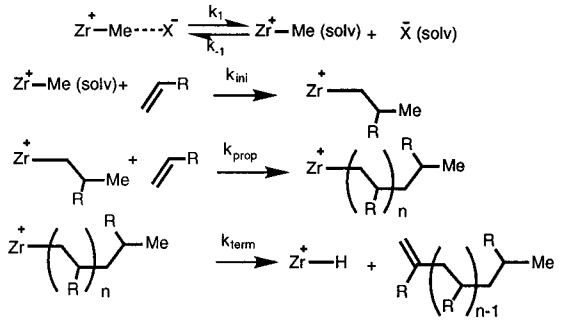

a distribution of activating species, further complicate the analysis because they may further speciate the catalytic centers.

Scheme 1, taken from the work of Siedle, Richardson, and co-workers,[5] illustrates a common, simple paradigm for metallocene-catalyzed polymerization of alkenes. Critical attributes of this model include the following: (1) solvent separation of ion-pairs precedes alkene insertion; (2) initiation and propagation proceed by simple bimolecular processes; and (3) β-hydride elimination is the primary chain termination process.

Many observations are difficult to reconcile with this simple model. For example, numerous reports of propene polymerization kinetics as catalyzed by Zr *ansa*-metallocenes with MAO cocatalysts indicate an apparent order in [alkene] that is >1.[6] Similar observations have been made for ethene and propene polymerization using unbridged bis-cyclopentadienyl[7] and monocyclopentadienyl[8] complexes as well as heterogeneous catalysts.[9] Varying orders in [monomer] have been reported for the rates of 1-hexene polymerization. Deffieux and co-workers[10] reported a first-order dependence with *rac*-(C_2H_4(1-indenyl)$_2$)$ZrCl_2$/MAO, similar to the order found by Chien and Gong[10b] for the same system. In contrast, Odian and co-workers[10c] found the order to vary from 1 to 1.4 for the *rac*-(dimethylsilyl)bis(4,5,6,7-tetrahydro-1-indenyl)$ZrCl_2$/MAO catalyst. Siedle and co-workers[10d] report a complex dependence of polymerization rate on [1-hexene] for the Cp_2ZrCl_2/MAO catalyst with an average order close to 2. Schrock's non-metallocene living polymerization catalysts for 1-hexene polymerization demonstrate first-order dependence of the rate on [1-hexene].[10c]

To accommodate the rate laws with orders in monomer greater than 1, several mechanistic refinements have been proposed. Prominent hypotheses include (1) the "trigger" model, in which two monomers are coordinated to the metal as the complexes passes through the insertion transition states,[8,11] and (2) various two-state models[6b,d,7,12] involving a fast propagating state and a slow propagating state for which the steady-state distribution of the catalyst between the two states depends on [alkene].

Chain termination processes in 1-alkene polymerization play a critical role in controlling polymer molecular weight and vary dramatically with the structure of the catalyst[13] and the nature of the 1-alkene.[14] Here we focus only on chain termination processes which yield unsaturated termini: unimolecular and bimolecular β-H transfer reactions. Following a 1,2 insertion β-H transfer yields a vinylidene end group, whereas a vinylene end group results from β-H transfer following a 2,1 insertion (or regioerror). Empirical data for propene polymerization catalyzed by *rac*-C_2H_4(1-indenyl)$ZrCl_2$/MAO demonstrate that the ratio of vinylene end groups to vinylidene end groups is proportional to [alkene].[13a,b] Chain termination processes that depend on alkene concentration yield saturation-like behavior in terms of the increase of polymer molecular weight with increased alkene concentration. Such data invariably are interpreted as indicating that vinylidene end groups arise from unimolecular β-hydride elimination (β-H transfer to metal) after a 1,2 insertion, whereas vinylene end groups arise from bimolecular β-H elimination (chain transfer to monomer) following a 2,1 insertion of propene.[13a] It is not obvious why the bulkier secondary alkyl must associate another monomer to terminate whereas the primary alkyl does not. For 1-hexene polymerization as catalyzed by *rac*-(C_2H_4(1-indenyl)$_2$)$ZrCl_2$/MAO, Deffieux *et alia*[10a] report that polymer molecular weights are independent of [1-hexene], whereas Odian et al.[10c] find that the molecular weights vary with [1-hexene] in a complex way. Furthermore, they report that the frequencies of vinylidene and vinylene end groups both depend on [1-hexene] but that the orders change with temperature, suggesting that both unimolecular and bimolecular pathways for β-H transfer following either 1,2 or 2,1 insertions may occur.

To resolve some of these outstanding issues, we have undertaken detailed kinetic studies of metallocene-catalyzed alkene polymerization. Recently, we reported a method for determining active site concentrations in metallocene-catalyzed alkene polymerizations (Scheme 2).[3a] This method consists of quenching the polymerization reaction with the concomitant introduction of a D label into the polymer. Only propagating species, such as **1***, are monitored because the deuteriomethane produced by reaction of **1** with MeOD is lost in workup. The time dependence of the appearance of label in the polymer reveals the kinetics of the initiation step, i.e., the conversion of **1** into **1***. The chemical shifts of the label determined by ^{2}H NMR

(4) Sinn, H.; Kaminsky, W. *Adv. Organomet. Chem.* **1980**, *18*, 99−149.
(5) Richardson, D. E.; Alameddin, N. G.; Ryan, M. F.; Hayes, T.; Eyler, J. R.; Siedle, A. R. *J. Am. Chem. Soc.* **1996**, *118*, 11244−11253.
(6) (a) Jüngling, S.; Müllhaupt, R.; Stehling, U.; Brintzinger, H.-H.; Fischer, D.; Langhauser, F. *Macromol. Symp.* **1995**, *97*, 205−216. (b) Jüngling, S.; Mülhaupt, R.; Stehling, U.; Brintzinger, H.-H.; Fischer, D.; Langhauser, F. *J. Polym. Sci.: Part A, Polym. Chem.* **1995**, *33*, 1305−1317. (c) Herfert, N.; Fink, G. *Makromol. Chem., Macromol. Symp.* **1993**, *66*, 157−178. (d) Wester, T. S.; Johnsen, H.; Kittilsen, P.; Rytter, E. *Macromol. Chem. Phys.* **1998**, *199*, 1989−2004.
(7) Thorshaug, K.; Støvneng, J. A.; Rytter, E.; Ystenes, M. *Macromolecules* **1998**, *31*, 7149−7165.
(8) Chien, J. C. W.; Yu, Z.; Marques, M. M.; Flores, J.; Rausch, M. D. *J. Polym. Sci.: Part A, Polym. Chem.* **1998**, *36*, 319−328.
(9) (a) Pino, P.; Rotzinger, B.; von Achenbach, E. *Makromol. Chem. Suppl.* **1985**, *13*, 105−122. (b) Kissin, Y. V.; Mink, R. I.; Nowlin, T. E. *J. Polym. Sci.: Part A, Polym. Chem.* **1999**, *37*, 4255−4272.
(10) (a) Coevoet, D.; Cramail, H.; Deffieux, A. *Macromol. Chem. Phys.* **1996**, *197*, 855−867. (b) Chien, J. C. W.; Gong, B. *N. J. Polym. Sci.: Part A, Polym. Sci.* **1993**, *31*, 1747−1754. (c) Zhao, X.; Odian, G.; Rossi, A. *J. Polym. Sci.: Part A, Polym. Sci.* **2000**, *38*, 3802−3811. (d) Siedle, A. R.; Lamanna, W. M.; Olofson, J. M.; Nerad, B. A.; Newmark, R. A. *Selectivity in Catalysis*; ACS Symposium Series 517; American Chemical Society: Washington, DC, 1993; pp 156−167. (e) Mehrkhodavandi, P.; Bonitatebus, P. J., Jr.; Schrock, R. R. *J. Am. Chem. Soc.* **2000**, *122*, 7841−7842.
(11) (a) Ystenes, M. *J. Catal.* **1991**, *129*, 383−401. (b) Ystenes, M. *Makromol. Chem., Macromol. Symp.* **1993**, *66*, 71−81. (c) Muñoz-Escalona, A.; Ramos, J.; Cruz, V.; Martinez-Salazar, J. *J. Polym. Sci.: Part A, Polym. Sci.* **2000**, *38*, 571−582.
(12) (a) Fait, A.; Resconi, L.; Guerra, G.; Corradini, P. *Macromolecules* **1999**, *32*, 2104−2109. (b) Busico, V.; Cipullo, R.; Chadwick, J. C.; Modder, J. F.; Sudmeijer, O. *Macromolecules* **1994**, *27*, 7538−7543. (c) Tsutsui, T.; Kashiwa, N.; Mizuno, A. *Makromol. Chem. Rapid Commun.* **1990**, *11*, 565−572.
(13) (a) Resconi, L.; Camurati, I.; Sudmeijer, O. *Top. Catal.* **1999**, *7*, 145−163. (b) Resconi, L.; Piemontesi, F.; Camurati, I.; Balboni, D.; Sironi, A.; Moret, M.; Rychlicki, H.; Zeigler, R. *Organometallics* **1996**, *15*, 5046−5059. (c) Resconi, L; Fait, A.; Piemontesi, F.; Colonnesi, M.; Rychlicki, H.; Zeigler, R. *Macromolecules* **1995**, *28*, 6667−6676. (d) Busico, V.; Cipullo, R.; Chadwick, J. C.; Modder, J. F.; Sudmeijer, O. *Macromolecules* **1994**, *27*, 7538−7543.
(14) (a) Thorshaug, K.; Rytter, E.; Ystenes, M. *Macromol. Rapid Commun.* **1997**, *18*, 715−722. (b) Kim, I.; Zhou, J.-M.; Chung, H. *J. Polym. Sci.: Part A, Polym. Chem.* **2000**, *38*, 1687−1697.

Scheme 2

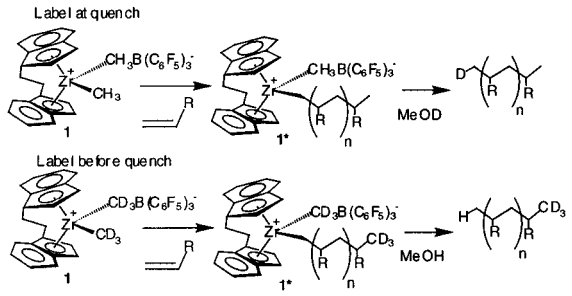

spectra of the labeled polymer further distinguish among the types (primary, secondary, allylic, vinylic, etc.) of Zr−alkyls that undergo methanolysis and, hence, the nature of the propagating species. For example, reaction of **1*** or any other primary alkyl−Zr bond with MeOD yields a labeled methyl group.[15]

We seek to strengthen our understanding of key issues in alkene polymerization via fundamental kinetic studies. In this paper, we demonstrate the application of active site counting methodology to the determination of initiation, propagation, and termination rate laws and activation parameters for the polymerization of 1-hexene as catalyzed by the contact ion-pair [*rac*-(C_2H_4(1-indenyl)$_2$)ZrMe][MeB(C_6F_5)$_3$] (**1**) in toluene solution.

Experimental Methods

General Procedures. All experiments were performed under air- and moisture-free conditions using a circulating nitrogen-filled glovebox operating at <0.2 ppm oxygen or under nitrogen using standard Schlenk line techniques. Toluene solvent for polymerization was stored in a stainless steel solvent reservoir under dinitrogen pressure (5−50 psig). Upon dispensing, the solvent passed through a column of activated alumina followed by a column of supported copper catalyst (Q-5). Benzene was purified by distillation with Na and benzophenone. Routine NMR characterization experiments were performed on Bruker AC-250, AC-300, Unity-500, and Inova-500 NMR spectrometers. ^{2}H NMR(77 MHz) spectra for initiation kinetics were recorded on a Unity-500 NMR spectrometer and referenced to the chemical shift of benzene (7.15 ppm). Gel permeation chromatography was performed on a Waters 150C high-temperature instrument by Dr. Judy Gunderson of Dow Chemical using a polystyrene/polyethene universal calibration. All molecular weights were reported as polyethene apparent molecular weights. FT-IR measurements were recorded with the ReactIR 1000 and React MP Mobile spectrometer.

1-Hexene was purified by distillation from Na/K alloy. Tris-(pentafluorophenyl)borane B(C_6F_5)$_3$ was obtained as a solid from Dow Chemical or prepared according to the literature procedures.[16] *rac*-(C_2H_4-(1-indenyl)$_2$)ZrMe_2 was synthesized by published methods.[17] [PhNMe_3]-[MeB(C_6F_5)$_3$] was obtained from Mr. Donald W. Carpenetti, II, and Prof. Charles P. Casey. MeOH and MeOD were used as received.

Microstructure Analysis by NMR Measurements. ^{1}H NMR and ^{13}C NMR spectra of poly-1-hexene were obtained in $CDCl_3$ solution at 24 °C on a UNITY 500 MHz spectrometer. A T_1 determination by the inversion recovery method was carried out for each sample. The ^{1}H NMR spectra were recorded at 500 MHz using 15 s delays between calibrated 90° pulses for 128 transients. The ^{13}C NMR spectra were obtained at 125 MHz with inverse gated decoupling using 12 s delays between calibrated 90° pulses. An acquisition time of 3 s was used, and 132K points were recorded. A total of 512 transients were obtained in 2 h. The two-dimensional INADEQUATE[18] data were obtained with 256 increments in the double-quantum dimension and 32 transients of 8K points per increment. A spectral width of 20 kHz in both dimensions was used, and J_{C-C} = 40 Hz.

Synthesis of ^{13}C-Labeled 1-Hexene.[19] A solution of triphenylphosphine (9.23 g, 0.0352 mol) in 18 mL of toluene was cooled to −10 °C. Methyl-*^{13}C* iodide (4.8 g, 0.0336 mol) was added to the solution. After 3 days a solid was formed. The solvent was removed, leaving 14.0 g of (methyl-*^{13}C*)triphenylphosphonium iodide, which was dissolved in 30 mL of dimethyl sulfoxide (DMSO). Sodium hydride (0.84 g, 0.035 mol) was reacted with 15 mL of DMSO at 70 °C for 45 min, resulting in a yellow solution. The reaction was cooled with an ice bath. The (methyl-*^{13}C*)triphenylphosphonium iodide in DMSO was added to the cooled solution to form the yellow ylide. Freshly distilled valeraldehyde (3.6 mL, 0.0336 mol) was added slowly to the reaction mixture at 0 °C. After the reaction was stirred at room temperature for 45 min, most of the ^{13}C-labeled 1-hexene was obtained by distillation. The remaining 1-hexene was recovered by vacuum transfer. A total of 2.44 g (85.5% yield) of ^{13}C-labeled 1-hexene was recovered.

^{1}H NMR (300 MHz, $CDCl_3$): δ 5.82 (m, 1H), 4.99 (m, J_{H-C} = 153 Hz, 1H), 4.93 (m, J_{H-C} = 153 Hz, 1H), 2.05 (m, 2H), 1.34 (m, 4H), 0.90 (t, 3H).

Initiation Kinetics by Automated Quench-Flow Techniques. Initiation kinetics were determined in a quench-flow apparatus.[20] Three toluene solutions, *rac*-(C_2H_4(1-indenyl)$_2$)ZrMe_2, 1-hexene with 1-hexene with B(C_6F_5)$_3$, B(C_6F_5)$_3$, and MeOD, were injected into the apparatus (typical concentrations: 8.0×10^{-4} M, 2.0 M, 8.0×10^{-4} M, and 1.0 M, respectively). The reaction was initiated by mixing the *rac*-(C_2H_4-(1-indenyl)$_2$)ZrMe_2 and 1-hexene/B(C_6F_5)$_3$ solutions together. The polymerization was quenched after a known time (typically 5−70 s) with the addition of MeOD. The temperature of the reaction was held constant with a silicone oil bath. The solution was collected, and volatiles were removed. A small volume of hexanes was added, and the solution was stirred overnight. The polymer solution was purified by passage through a 3 cm long × 1.5 cm diameter activated alumina column, using hexanes as the eluent (5 × 6 mL). The solvent was then removed to isolate the polymer. The polymer was then dissolved in 0.67 mL of benzene, and 0.32 μL of $CDCl_3$ was added as an internal standard. ^{2}H NMR spectra of the polymer solutions (5 mm tube, 77 MHz, 2 s acquisition time, 2 s relaxation delay, 90° pulse, 128 acquisitions, 8K data points, 3 Hz line broadening) were collected, and the fraction of active sites was determined by integration of the polymer resonances against that of the internal standard.

Initiation and Propagation Kinetics by Manual Quench. In a typical experiment, a round-bottom flask equipped with a stir bar inside a glovebox was charged with 25.6 mg (50 μmol) of B(C_6F_5)$_3$ in 58 mL of a 1 M 1-hexene solution in toluene and capped with a septum. After the solution was cooled to 0 °C in an ice bath outside the glovebox, 2 mL of 8.3×10^{-4} M *rac*-(C_2H_4(1-indenyl)$_2$)ZrMe_2 (18.9 mg, 50 μmol) was quickly injected into the solution. Reaction exotherms were less than 2 °C. The reaction length was timed using a stopwatch, and the reaction was quenched by injecting 1.0 mL of 5 M MeOD in toluene. All volatiles were then removed from the solution under reduced pressure, and the polymer was dissolved in 3−5 mL of hexane by stirring overnight. This polymer solution was then passed through an activated aluminum column to remove the quenched catalyst products. The column (3 cm long × 1.5 cm diameter) was rinsed with 6 × 5 mL of hexane, and the hexane was removed. The purified polymer was weighed. For initiation kinetics experiments, deuterium NMR samples were prepared by dissolving the purified polymer in 0.7 mL of C_6H_6 and adding $CDCl_3$ as an internal standard.

Propagation and Termination Kinetics by Automated Quench-Flow Techniques. Propagation kinetics were determined in a quench-

(15) For a related use of D-labeling, see: Chirik, P. J.; Day, M. W.; Labinger, J. A.; Bercaw, J. E. *J. Am. Chem. Soc.* **1999**, *121*, 10308−10317.

(16) (a) Massey, A. G.; Park, A. J. *J. Organomet. Chem.* **1964**, *2*, 245−250. (b) Massey, A. G.; Park, A. J. *J. Organomet. Chem.* **1966**, *5*, 218−225.

(17) (a) Wild, F. R. W. P.; Wasiucionek, M.; Huttner, G.; Brintzinger, H.-H. *J. Organomet. Chem.* **1985**, *288*, 63−67. (b) Collins, S.; Kuntz, B. A.; Taylor, N. J.; Ward, D. G. *J. Organomet. Chem.* **1988**, *342*, 21−29. (c) Chien, J. C. W.; Tsai, W.-M.; Rausch, M. D. *J. Am. Chem. Soc.* **1991**, *113*, 8570−8571.

(18) (a) Bax, A.; Freeman, R.; Frenkiel, T. A. *J. Am. Chem. Soc.* **1981**, *103*, 2101−2104. (b) Buddrus, J.; Bauer, J. *Angew. Chem., Int. Ed. Engl.* **1987**, *26*, 625−643.

(19) (a) Greenwald, R.; Chaykovsky, M.; Corey, E. J. *J. Org. Chem.* **1963**, *28*, 1128. (b) Gajewski, J. J.; Peterson, K. B.; Kagel, J. R; Huang, Y. C. *J. J. Am. Chem. Soc.* **1989**, *111*, 9078.

(20) White, C. B.; Rosaaen, K. A.; Landis, C. R., manuscript in preparation.

flow apparatus. Three toluene solutions, *rac*-(C_2H_4(1-indenyl)$_2$)$ZrMe_2$ (8.0×10^{-4} M), 1-hexene (2.0 M)/$B(C_6F_5)_3$ (8.0×10^{-1} M), and MeOH (1.0 M), were injected into the sample loops of a quenched-flow apparatus. The reaction was initiated by mixing the *rac*-(C_2H_4(1-indenyl)$_2$)$ZrMe_2$ and 1-hexene/$B(C_6F_5)_3$ solutions together. The polymerization was quenched after a known time (typically 5−120 s) by the addition of MeOD. The temperature of the reaction was held constant with a silicone oil bath. The polymer solution was collected, and the volatiles were removed. A small volume of hexanes was added, and the solution was stirred overnight. The polymer solution was purified by passage through a 3 cm long × 1.5 cm diameter activated alumina column, using hexanes as the eluent (5 × 6 mL). The purified polymer was then weighed to determine the amount of 1-hexene reacted.

The polymer samples were dissolved in 0.67 mL of benzene-d_6 with 1.8 μL of 4-fluoroanisole added as an internal standard. ^{1}H NMR spectra of the polymer solutions (5 mm tube, 500.3 MHz, 5 s acquisition time, 5 s relaxation delay, 60° pulse, 128 acquisitions, 64K data points) were collected, and the fractions of vinylidene- and vinylene-terminated polymer were determined by integration of the peaks versus the internal standard.

Kinetic Measurements with IR Spectroscopy. In a typical experiment, 1-hexene (7.5 mL, 60 mmol) was added to a Schlenk flask followed by toluene addition to yield a total volume of 58 mL. $B(C_6F_5)_3$ (24.57 mg, 0.048 mmol) was added to the solution. Separately, *rac*-(C_2H_4(1-indenyl)$_2$)$ZrMe_2$ **1** (18.13 mg, 0.048 mmol) was dissolved in 2 mL of toluene and transferred into a 5 mL gastight syringe. The reaction was carried out on in a flask fitted with the DiComp probe of a ReactIR infrared spectrometer. An empty flask was used to collect the reference spectrum. The solution of 1-hexene and $B(C_6F_5)_3$ in toluene was transferred into the reactor. Reaction was initiated by injection of a solution of *rac*-(C_2H_4(1-indenyl)$_2$)$ZrMe_2$ to the stirred reactor. Reaction progress was monitored by following the decrease in 1-hexene absorbances at 911 and 995 cm^{-1}. The profile of absorbance vs time was fit to a single exponential with two adjustable parameters: the rate constant and the absorbance at infinite time.

Stopped-Flow Experiments. A Hi-Tech Scientific SF-40 stopped-flow instrument equipped with an anaerobic manifold and interfaced with a glovebox was used for all UV−vis stopped-flow experiments. The formation of the ion-pair creates a dark yellow solution, λ_{max} = 432 nm. Typical shot volumes were 0.5 mL. The reaction rate was faster than the dead time of the instrument (4 ms) at −32 °C, with final concentrations of *rac*-(C_2H_4(1-indenyl)$_2$)$ZrMe_2$ and $B(C_6F_5)_3$ at 2.08×10^{-4} M in toluene.

Runge−Kutta Simulations. Numerical simulations of the polymerization were calculated using a program written in Mathcad 8. These simulations used the built-in Mathcad algorithm called rkadapt. This algorithm employs a fourth-order Runge−Kutta solver for differential equations that includes variable-sized steps during the iteration process. The rkadapt routine takes an array of differential equations and an array of initial concentrations and calculates the concentrations of species after a specified time:

$$\text{Rate}_i = k_i\,[\text{monomer}]\,[\text{ZrMe}] + k_{iH}\,[\text{monomer}]\,[\text{ZrH}]$$

$$\text{Rate}_p = k_p\,[\text{Zr}\cdot\text{polymer}_n]$$

$$\text{Rate}_t = k_{\text{vinylene}}\,[\text{Zr}\cdot\text{polymer}_n]\,[\text{monomer}] + k_{\text{vinylidene}}\,[\text{Zr}\cdot\text{polymer}_n]$$

Rate constants and rate laws are defined in the main text. In all of the simulations, the rate constant for initiation (k_{iH}) of [*rac*-(C_2H_4-(1-indenyl)$_2$)ZrMe][$MeB(C_6F_5)_3$] was set to be 1000 times larger than the rate constant for initiation at ZrMe. However, the actual value of this rate constant has little effect on the computed distributions. Termination was assumed to proceed by a process either apparently first or zero order in [monomer]. These termination processes yield alkene-terminated polymers (with *n* incorporated monomers) and either a catalyst with one monomer attached or a metal hydride catalyst, respectively.

With this kinetic scenario, an array of differential equations describing changes in concentrations of species in solution is programmatically constructed. One must account for a number of species. These include monomer, catalyst as metal−alkyl and metal−hydride, catalyst with growing polymer of *n* insertions, and terminated polymer chains *n* monomers in length. For a simulation that follows 1000 insertions, this requires a concentration array and an array of differential equations with 2003 elements each.

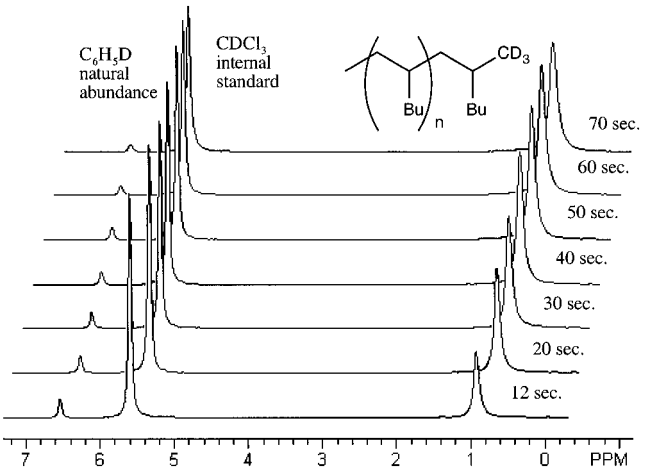

Figure 1. ^{2}H NMR (77 MHz) spectra of ^{2}H-labeled poly-1-hexene as a function of reaction time (reaction performed at 0 °C, [**1**-d_6]$_0$ = 8.3×10^{-4} M, [1-hexene]$_0$ = 1.0 M, toluene solvent; ^{2}H NMR spectra of purified polymer taken in benzene solvent).

After calculating the concentration of each species in solution at a given reaction time, the molecular weight distribution is calculated. For this distribution, the concentration of each terminated polymer chain is added to the propagating chain of equal length. Using the molecular weight of the monomer, the weight of each combined concentration can be calculated. In this way, a plot of mass versus log(MW) is constructed.

To directly compare the calculated and experimental molecular weight distributions, some manipulations of the GPC plots were necessary. First, the data were hand-digitized and entered into a spreadsheet. Next, the ethene apparent molecular weights were converted into poly-1-hexene molecular weights by multiplication by 3. The molecular weight metrics M_w, M_n, and M_w/M_n were computed from the converted molecular weights. Finally, both experimental and calculated intensities were normalized for comparison.

Results

Initiation Kinetics. In this work, we define initiation to be the first insertion of alkene into the Zr−Me bond of **1**. As we have shown previously,[3a] the initiation rate can be monitored by time-resolved quench-flow studies of the incorporation of deuterium labels into polymer. These deuterium labels may originate either from use of MeOD as quench or from deuterium-labeling of the methyl groups of **1** (Scheme 2). After initial exposure of **1** to 1-hexene, the fraction of active sites (i.e., the ratio [**1***]/[**1**]$_0$) grows by a first-order process to reach a maximum value ca. 0.9 (see Figures 1 and 2). Analysis of the growth of label in the polymer according to eq 1 yields the observed initiation rate constant, k_i^{obs}:

$$\frac{\partial[\mathbf{1}^*]}{\partial t} = k_i^{obs}\,[\mathbf{1}] \Rightarrow \ln\left(\frac{[\mathbf{1}^*]}{[\mathbf{1}]_0}\right) = k_i^{obs} t + \text{const} \qquad (1)$$

Whether one labels with D at the quench or begins with CD_3-labeled **1**, the same values of k_i^{obs} are obtained.[3a] Furthermore, only one of the two labeled CD_3 groups of **1** are incorporated into the polymer. The nature of the propagating species is unambiguously identified as a primary alkyl resulting from methanolysis of **1*** via the observation of label in terminal methyl positions, only (see Figure 1), and by ^{13}C NMR (vide infra). A complete listing of initiation kinetic data is provided

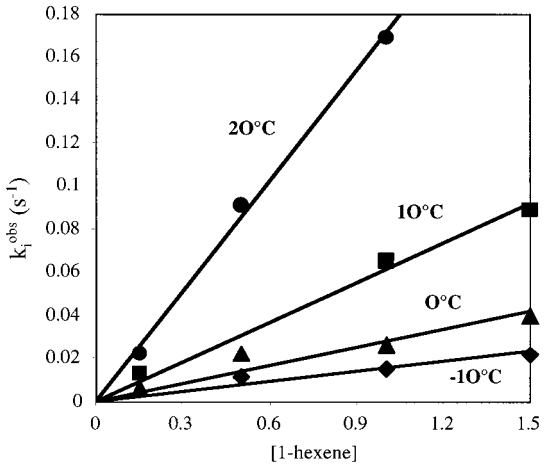

Figure 2. Plots of observed initiation rate constants vs [1-hexene] at various temperatures (toluene, $[\mathbf{1}]_0 = 8.3 \times 10^{-4}$ M, 1-hexene conversion <12% for all reactions, points represent observed data and solid lines represent results of linear regression).

in Table 1. At 0 °C with 1.0 M concentration of 1-hexene, the half-life for initiation is about 21 s. The initiation rate constant, k_i^{obs}, is unaffected by the addition of excess borane or whether the catalyst is the isolated complex **1** or is generated in situ by mixing of $B(C_6F_5)_3$ and *rac*-$(C_2H_4(1\text{-indenyl})_2)ZrMe_2$. Over the temperature range of −10 to 30 °C, k_i^{obs} increases linearly with [1-hexene], thus establishing the initiation rate law of eq 2 (see Figure 2).

$$\frac{\partial[\mathbf{1}^*]}{\partial t} = k_i\,[\mathbf{1}]\,[\text{1-hexene}] \qquad (2)$$

$$\Delta H^{\ddagger} = 11.5 \pm 1.5 \text{ kcal/mol} \quad \Delta S^{\ddagger} = -24 \pm 6 \text{ cal/(mol K)}$$

In separate stopped-flow experiments, the reaction of 0.2 mM $B(C_6F_5)_3$ and 0.2 mM *rac*-$(C_2H_4(1\text{-indenyl})_2)ZrMe_2$ (see below) in toluene at −32 °C was found to be faster than the mixing time of the stopped-flow instrument. This result places an upper limit on the reaction half-life of approximately 5 ms at −32 °C; methide abstraction from **1** by $B(C_6F_5)_3$ is much faster than initiation. Previous data reported by Marks and co-workers[1b,21] suggest that borane association should have a very low activation enthalpy (<4 kcal/mol).

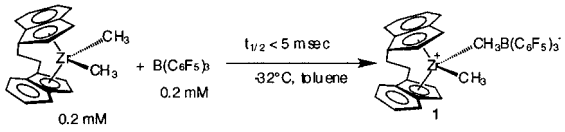

Propagation Kinetics. Catalytic polymerization rates may be monitored conveniently by quenched-flow methods or by IR spectroscopy. Quenched-flow studies measure the accumulation of polymer mass with time, whereas IR spectroscopy monitors the disappearance of 1-hexene. Quenched-flow studies were performed either in a specially constructed rapid quench-flow apparatus that is interfaced with an inert atmosphere glovebox[20] or in common glassware. Propagation kinetic data measured by all methods are provided in Table 1.

Quenched-flow polymerizations of 1-hexene in toluene solution were performed with short quench times such that [1-hexene] changed by less than 10% and exotherms <1 °C were effected. Representative data are shown in Figure 3. As the curvature of the polymer mass vs time plot in Figure 3 clearly indicates, accumulation of polymer mass accelerates with time during the initial reaction period. Such acceleration suggests that propagation is faster than initiation. Assume that (1) initiation is irreversible, (2) [1-hexene] is constant over the reaction time, and (3) the intrinsic rate constants and orders of all subsequent propagation steps are the same. Then the kinetic scenario of Scheme 3 leads to the integrated rate law shown in eq 4 for the growth of polymer mass with time. Note that this rate law does not assume an order for [1-hexene] dependence of the propagation rate (eq 3).

Scheme 3

$$\mathbf{1} + \text{1-hexene} \xrightarrow{k_i} \mathbf{1}^*$$

$$\mathbf{1}^* \xrightarrow{k_p^{obs}} \mathbf{1}^*_1 \xrightarrow{k_p^{obs}} \mathbf{1}^*_2 \xrightarrow{k_p^{obs}} \mathbf{1}^*_3 \cdots$$

$$\text{assume} \quad \frac{\partial[\text{1-hexene}]}{\partial t} = -k_p^{obs}\,[\mathbf{1}^*] \qquad (3)$$

$$\text{mass}(t) = \text{volume}(84.16)k_p^{obs}\,[1]_0 \times \left(t + \frac{1}{k_i\,[\text{1-hexene}]_0}\,e^{-k_i[\text{1-hexene}]_0 t} - \frac{1}{k_i\,[\text{1-hexene}]_0}\right) \qquad (4)$$

Analysis of the initial rates of polymerization according to eq 4 with the independently determined value of the initiation rate constant (k_i) held constant and variation of the fitting parameter, k_p^{obs}, leads to an excellent simulation of the experimental data. From the first-order dependence of k_p^{obs} on $[\text{1-hexene}]_0$ (0.15−1.5 M), the following rate law is determined (eq 5). The propagation rate is unaffected by the addition of excess borane (1−4 equiv of $B(C_6F_5)_3$ per Zr).

$$\frac{\partial[\text{1-hexene}]}{\partial t} = k_p\,[\mathbf{1}^*]\,[\text{1-hexene}] \qquad (5)$$

The rate data provided so far address the reaction in its initial stages, only. Do these empirical rate data describe 1-hexene polymerization kinetics throughout the complete conversion of monomer into polymer? For these measurements we turn to experiments in which the complete time course of 1-hexene consumption is monitored. At 0 °C, in situ infrared spectroscopy was used to monitor 1-hexene consumption. These measurements were performed under conditions such that exotherms are controlled to <1 °C. As shown in Figure 4, the disappearance of 1-hexene is first order in [1-hexene] over 95% consumption of monomer. The only significant deviation from this behavior occurs during the first 90 s, when catalyst initiation is incomplete. Values of k_p^{obs} resulting from the 1-hexene disappearance kinetics as a function of [Zr] lead to the same propagation rate law as determined by quench-flow studies (see Table 1).

Similarly, the rate of reaction may be followed through ca. 75% consumption of 1-hexene by quenched-flow studies at long reaction times (Figure 5). These studies also demonstrate a simple first-order decay of [1-hexene] vs time.

In summary, three methods have been used to determine the propagation rate law. Similar rate laws and rate constants are obtained by the three methods, which attests to the robustness of the kinetic scheme. All propagation data are consistent with a constant concentration of Zr active sites throughout the bulk of the reaction (excluding the early catalyst initiation stage) and do not support significant, irreversible "death" of the active catalyst under the conditions studied. Over the temperature range

(21) (a) Deck, P. A.; Beswick, C. L.; Marks, T. J. *J. Am. Chem. Soc.* **1998**, *120*, 1772−1784. (b) Luo, L.; Marks, T. J. *Topics in Catalysis*; Baltzer: Amsterdam, 1999; Vol. 7, pp 97−106.

Table 1. Summary of Initiation and Propagation Kinetics Measurements

$[Zr]_{tot}$ (M)	$[B(C_6F_5)_3]$ (M)	[1-hexene] (M)	temp (°C)	k_i (M^{-1} s^{-1})	k_p (M^{-1} s^{-1})	mean k_i (M^{-1} s^{-1})	mean k_p (M^{-1} s^{-1})
8.3×10^{-4}	8.3×10^{-4}	5.0×10^{-1}	−10	2.3×10^{-2}	2.0	$1.8 \times 10^{-2} \pm 4.6 \times 10^{-3}$	$1.7 \pm 3.9 \times 10^{-1}$
8.3×10^{-4}	8.3×10^{-4}	1.0	−10	1.5×10^{-2}	1.8		
8.3×10^{-4}	8.3×10^{-4}	1.5	−10	1.5×10^{-2}	1.3		
8.3×10^{-4}	8.3×10^{-4}	1.5×10^{-1}	0	4.2×10^{-2}	2.8	$3.3 \times 10^{-2} \pm 9.2 \times 10^{-3}$	$2.2 \pm 4.0 \times 10^{-1}$
8.3×10^{-4}	8.3×10^{-4}	5.0×10^{-1}	0	4.5×10^{-2}	2.9		
4.0×10^{-4}	4.0×10^{-4}	1.0	0	4.5×10^{-2}	1.9		
6.0×10^{-4}	6.0×10^{-4}	1.0	0	4.5×10^{-2}	2.1		
8.0×10^{-4}	8.0×10^{-44}	1.0	0	4.5×10^{-2}	2.1		
8.3×10^{-4}	8.3×10^{-4}	1.0	0	2.6×10^{-2} 2.3			
8.3×10^{-4}	8.3×10^{-4}	1.0	0	2.7×10^{-2}	1.9		
1.0×10^{-3}	1.0×10^{-3}	1.0	0	-	1.9		
8.3×10^{-4}	8.3×10^{-4}	1.5	0	2.7×10^{-2}	1.9		
8.3×10^{-4}	8.3×10^{-4}	1.5×10^{-1}	10	8.6×10^{-2}	4.6	$7.0 \times 10^{-2} \pm 1.4 \times 10^{-2}$	$3.6 \pm 9.2 \times 10^{-1}$
8.3×10^{-4}	8.3×10^{-4}	1.0	10	6.510^{-2}	3.2		
8.3×10^{-4}	8.3×10^{-4}	1.5	10	5.9×10^{-2}	2.9		
8.3×10^{-4}	8.3×10^{-4}	1.5×10^{-1}	20	1.5×10^{-1}	7.4	$1.7 \times 10^{-1} \pm 1.8 \times 10^{-2}$	6.3 ± 0.6
8.3×10^{-4}	8.3×10^{-4}	5.0×10^{-1}	20	1.8×10^{-1}	5.4		
8.3×10^{-4}	8.3×10^{-4}	1.0	20	1.7×10^{-1}	6.0		
8.3×10^{-4}	8.3×10^{-4}	1.5×10^{-1}	30	3.3×10^{-1}	11	3.3×10^{-1}	11
8.3×10^{-4}	8.3×10^{-4}	1.5×10^{-1}	50		15		17 ± 1.4
8.3×10^{-4}	8.3×10^{-4}	0.50	50		16		
8.3×10^{-4}	8.3×10^{-4}	1.0	50		17		
8.3×10^{-4}	8.3×10^{-4}	1.5	50		19		

initiation		propagation	
$\Delta H^{\ddagger}$	11.2 ± 1.5 kcal/mol	$\Delta H^{\ddagger}$	6.4 ± 1.5 kcal/mol
$\Delta S^{\ddagger}$	-24 ± 5 cal/(mol K)	$\Delta S^{\ddagger}$	-33 ± 5 cal/(mol K)
$k_i(298)$	0.25 M^{-1} s^{-1}	$k_p(298)$	8.1 M^{-1} s^{-1}

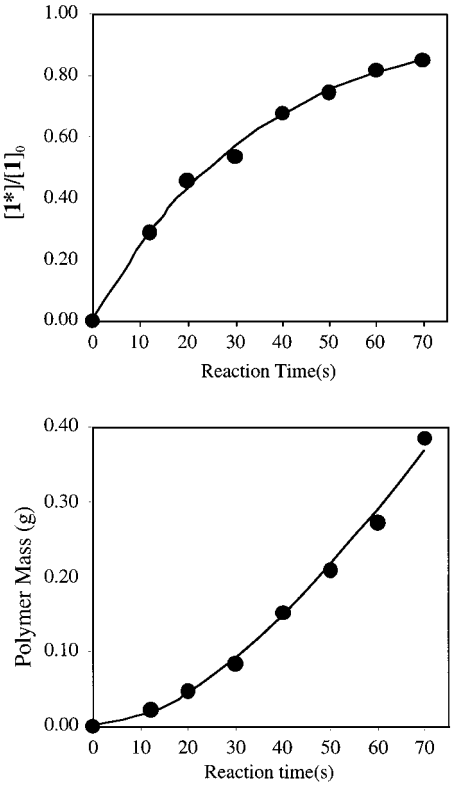

Figure 3. Calculated vs observed data for initiation (top) and propagation (bottom). All conditions are identical to those of Figure 1; in the bottom plot, 0.4 g of polymer corresponds to 8% conversion of 1-hexene.

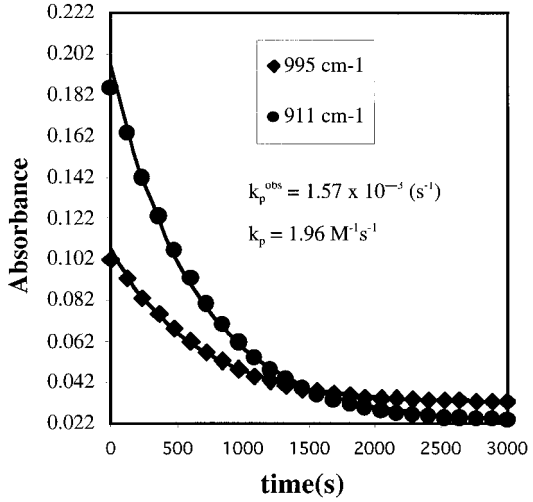

Figure 4. Kinetics of 1-hexene polymerization as monitored by IR spectroscopy (0 °C, toluene, $[\mathbf{1}]_0 = 8 \times 10^{-4}$ M, $[1\text{-hexene}]_0 = 1.0$ M, points represent observed data and the solid lines are fits to a single-exponential decay).

of −10 to 50 °C, the propagation activation parameters are $\Delta H^{\ddagger} = 6.4 \pm 1.5$ kcal/mol and $\Delta S^{\ddagger} = -33 \pm 6$ cal/(mol K).

In principle, propagation activity could be inhibited by increasing the concentration of the $MeB(C_6F_3)_3$ anion. For example, assume that a pre-equilibrium similar to Scheme 1 involving complete separation and solvation of the ion-pair **1** generates *free* $MeB(C_6F_5)_3^-$ and *rac*-$(C_2H_4(1\text{-indenyl})_2)ZrMe^+$ ions. If *rac*-$(C_2H_4(1\text{-indenyl})_2)Zr^+$ were the sole active species in polymerization, addition of salt containing the common anion, $MeB(C_6F_5)_3^-$, must depress the polymerization activity by shifting this pre-equilibrium toward **1**. We find that addition of 1−4 equiv of $[PhNMe_3][MeB(C_6F_5)_3]$ per Zr to catalytic reactions at 0 °C has no influence on the propagation rates as monitored by in situ IR spectroscopy throughout complete consumption of 1-hexene. This result conclusively demonstrates that free ions are not the principal propagating species. How-

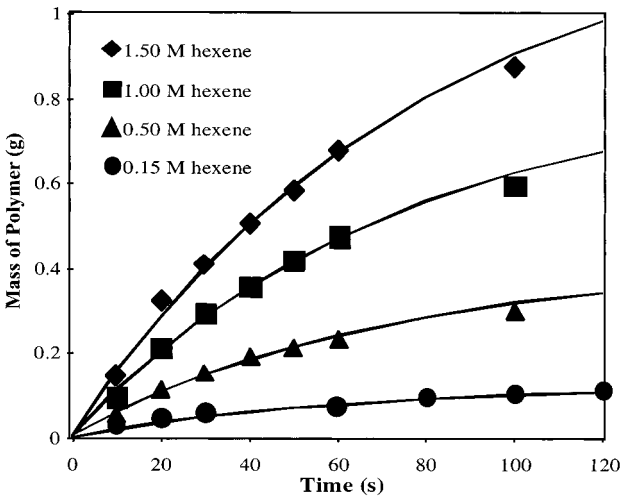

Figure 5. Polymerization progress as a function of time in toluene solution at different initial concentrations of 1-hexene. Each run exhibits 70−80% conversion of monomer at the 100 s time point ($[\mathbf{1}]_0 = 8.3 \times 10^{-4}$ M, $[B(C_6F_5)_3]_0 = 8.3 \times 10^{-4}$ M).

ever, these experiments do not exclude solvent-separated ion pairs (also known as loose ion-pairs) as the principal catalytic species.

Termination Kinetics. Polymerization of 1-hexene as catalyzed by **1** in toluene solution yields >99% isotactic poly-1-hexene with number-average molecular weights that range from ca. 2000 to 60 000. Two types of unsaturated end groups are observed in the ^{1}H NMR spectra of quenched polymers (Figure 6): vinylidene (δ 4.68 and 4.76 ppm) and vinylene end groups (δ 5.3 ppm). Conventional wisdom[2a] dictates that vinylidene resonances arise from termination after a 1,2 insertion, whereas vinylene resonances result from termination after a 2,1 insertion (Scheme 4). Less than 5% of the end groups correspond to mono- or trisubstituted alkenes, which are neglected in this analysis. At short reaction times, the concentrations of vinylidene and vinylene end groups accelerate with time, as expected for a catalyst in which initiation is slow (vide supra). In this time period, less than 10% of the monomer is polymerized, and the [1-hexene] is effectively constant. Analysis of the appearance of vinylidene and vinylene end groups with time (Figure 7), according to eq 6 and using the previously determined rate constants for initiation (k_i), yields the observed rate constants $k^{obs}_{vinylidene}$ and $k^{obs}_{vinylene}$.

$$\frac{\partial[\text{end group}]}{\partial t} = k_t^{obs}\,[\mathbf{1}]_0\left(t + \frac{1}{k_i\,[\text{1-hexene}]_0}\,e^{-k_i[\text{1-hexene}]_0 t} - \frac{1}{k_i\,[\text{1-hexene}]_0}\right) \quad (6)$$

The variation of $k^{obs}_{vinylene}$ and $k^{obs}_{vinylidene}$ with [1-hexene] reveals different fundamental rate laws for two termination products (Table 2). Whereas the rate of vinylidene formation is independent of [1-hexene], the rate of vinylene formation is first order in [1-hexene] (see Figures 8 and 9). The data also indicate a larger temperature dependence for the vinylidene observed rate constant than for the vinylene; logarithmic plots are shown in Figure 8 so that data for all temperatures can be shown on the same plot. Experimental data are consistent with the rate laws for termination that are provided below. The activation entropies for vinylene and vinylidene formation are consistent

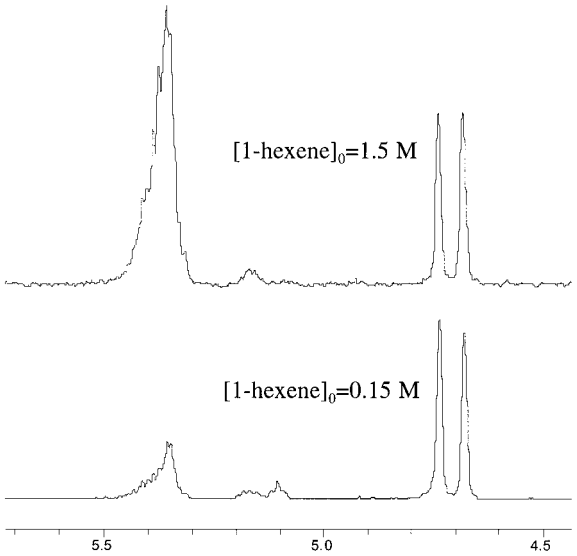

Figure 6. ^{1}H NMR (500 MHz) spectra of the vinyl regions of poly-1-hexene obtained at two different initial concentrations of 1-hexene (toluene, $[\mathbf{1}]_0 = 8.3 \times 10^{-4}$ M, 0 °C, ca. 8% conversion of 1-hexene).

Scheme 4

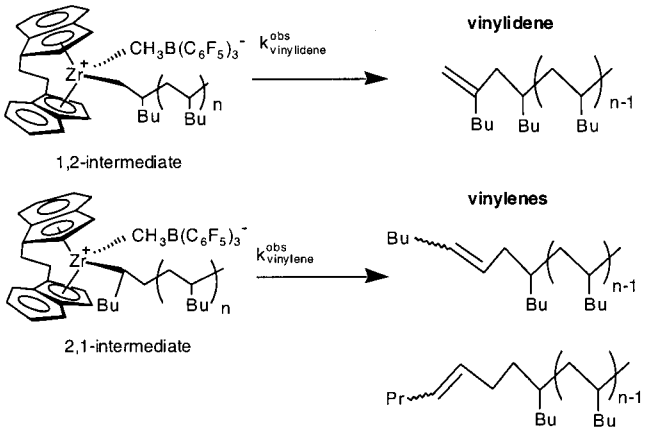

with bimolecular and unimolecular processes, respectively.

$$\frac{\partial[\text{vinylene}]}{\partial t} = k_{vinylene}\,[\mathbf{1}^*]\,[\text{1-hexene}] \quad (7)$$

$$k_{vinylene}(298\text{ K}) = 9.7 \times 10^{-3}\ \text{M}^{-1}\ \text{s}^{-1}$$

$$\Delta H^{\ddagger} = 9.7 \pm 1.2\ \text{kcal/mol} \qquad \Delta S^{\ddagger} = -35 \pm 4\ \text{cal/(mol K)}$$

$$\frac{\partial[\text{vinylidene}]}{\partial t} = k_{vinylidene}\,[\mathbf{1}^*] \quad (8)$$

$$k_{vinylidene}(298\text{ K}) = 1.3 \times 10^{-3}\ \text{s}^{-1}$$

$$\Delta H^{\ddagger} = 16.2 \pm 3\ \text{kcal/mol} \qquad \Delta S^{\ddagger} = -12 \pm 6\ \text{cal/(mol K)}$$

The dependence of the termination rates on [1-hexene] also can be probed by examining the influence of the [1-hexene]/[Zr] ratio on the distribution of end groups under conditions where all of the 1-hexene is converted into polymer. Consistent with the rate laws determined independently by quench-flow kinetics, we find that [vinylene]/[vinylidene] end groups increases linearly with increasing [1-hexene].

Modeling of Molecular Weight Distributions. Based on the empirical rate laws and kinetic parameters for catalytic polym-

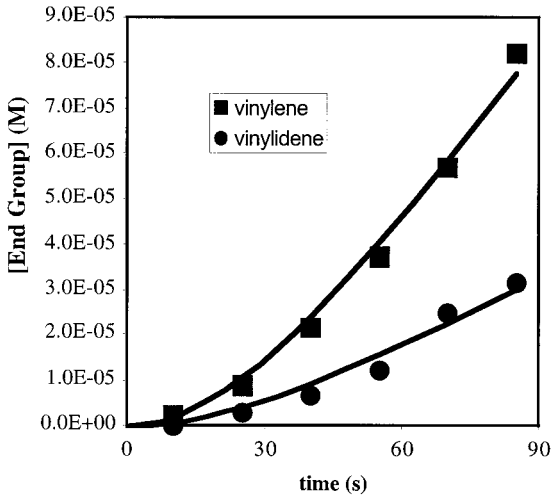

Figure 7. Demonstration of the time evolution of vinylene and vinylidene end groups (toluene solution, 0 °C, $[\mathbf{1}]_0 = 8.3 \times 10^{-4}$ M, [1-hexene] = 1.0 M, points represent experimental data and solid lines represent least-squares fit to eq 6).

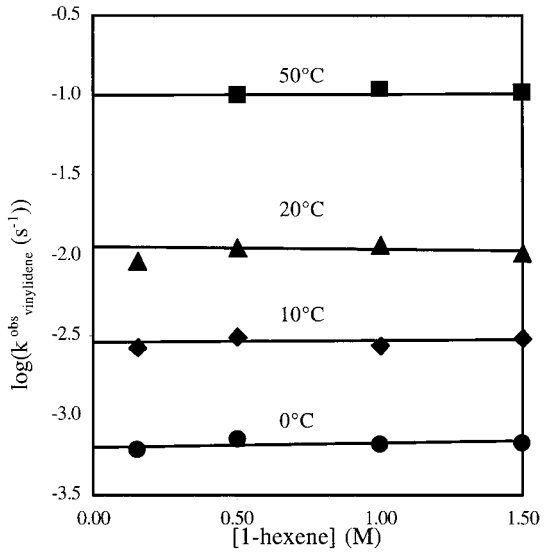

Figure 8. Plot of $\log(k^{obs}_{vinylidene})$ vs [1-hexene] at different temperatures for the formation of vinylidene end groups (toluene, $[\mathbf{1}]_0 = 8.3 \times 10^{-4}$ M, points represent experimental data and the solid lines are least-squares fits to the data; at 50 °C the [1-hexene] = 0.15 M point was excluded from the fit).

erization, it is possible to compute the polymer molecular weight distribution by kinetic modeling. We have used numerical integration of the empirical differential equations describing initiation, propagation, and termination to compute the total conversion of 1-hexene to poly-1-hexene and the molecular weight distribution of the polymer. One rate constant, the rate constant for re-initiation of chain growth following β-H elimination via insertion of 1-hexene into the Zr−H bond, was assumed to be >10-fold larger than the propagation rate constant. The results are compared with experimental molecular weight distributions as determined by gel permeation chromatography (GPC) in Figure 10. Good agreement is found for experimental and computed masses, polydispersities, and the qualitative shapes of the molecular weight distributions. However, the fit is not perfect, with a consistently lower observed M_n than computed and a broader distribution of molecular weights found experimentally. We attribute these differences to systematic errors in the GPC calibration of absolute molecular weights.

Polymer Microstructure via NMR Analysis. Natural abundance ^{13}C NMR spectra of poly-1-hexene obtained at 0 °C clearly reveal a highly isotactic polymer with no obvious defects due to stereoerrors, enchained 2,1 insertions, "3,1" insertions, or other errors.[22] Our interest in quantifying the occurrence of various errors and the origins of various end groups led us to synthesize 1-hexene that is 99% ^{13}C-labeled at the C-1 position. Polymerization of labeled 1-hexene (0 °C, $[\text{1-hexene}]_0 = 5.7$ M, $[\mathbf{1}] = 8 \times 10^{-4}$ M) to 60% conversion followed by quench with MeOD yielded poly-1-hexene, for which the ^{13}C NMR spectrum is shown in Figure 11. Analysis of this polymer by 1-D ^{13}C NMR, 2-D ^{13}C NMR INADEQUATE, 2-D ^{1}H−^{13}C HMBC NMR, and 1-D ^{1}H NMR spectroscopy led to the assignments which are summarized in Table 3 and Scheme 5. Our primary interest in analyzing the microstructure of ^{13}C-labeled 1-hexene was to determine if 2,1 regioerrors were enchained in the polymer. With a ^{13}C label at C-l, the occurrence of 2,1 regioerrors leads to ^{13}C labels on adjacent carbons which are detectable by splitting in standard 1-D ^{13}C NMR spectra or

Table 2. Kinetic Parameters for Termination Processes in 1-Hexene Polymerization

[Zr] (M)	[$B(C_6F_5)_3$] (M)	[1-hexene] (M)	temp (°C)	$k^{obs}_{vinylene}$ (s^{-1})	$k^{obs}_{vinylidene}$ (s^{-1})	$k^{obs}_{vinylene}$ (mean, s^{-1})	$k^{obs}_{vinylidene}$ (mean, s^{-1})
8.3×10^{-4}	8.3×10^{-4}	1.5×10^{-1}	0.0	1.8×10^{-3}	6.1×10^{-4}	$1.6 \times 10^{-3} \pm 2.4 \times 10^{-4}$	$6.6 \times 10^{-4} \pm 4.3 \times 10^{-5}$
8.3×10^{-4}	8.3×10^{-4}	5.0×10^{-1}	0.0	1.8×10^{-3}	7.1×10^{-4}		
8.3×10^{-4}	8.3×10^{-4}	1.0	0.0	1.7×10^{-3}	6.5×10^{-4}		
8.3×10^{-4}	8.3×10^{-4}	1.5	0.0	1.3×10^{-3}	6.8×10^{-4}		
8.3×10^{-4}	8.3×10^{-4}	1.5×10^{-1}	10.0	3.9×10^{-3}	2.7×10^{-3}	$3.5 \times 10^{-3} \pm 4.8 \times 10^{-4}$	$2.9 \times 10^{-3} \pm 2.1 \times 10^{-4}$
8.3×10^{-4}	8.3×10^{-4}	5.0×10^{-1}	10.0	4.0×10^{-3}	3.1×10^{-3}		
8.3×10^{-4}	8.3×10^{-4}	1.0	10.0	3.1×10^{-3}	2.7×10^{-3}		
8.3×10^{-4}	8.3×10^{-4}	1.5	10.0	3.1×10^{-3}	3.0×10^{-3}		
8.3×10^{-4}	8.3×10^{-4}	1.5×10^{-4}	20.0	6.9×10^{-3}	9.2×10^{-3}	$6.9 \times 10^{-3} \pm 6.0 \times 10^{-4}$	$1.1 \times 10^{-2} \pm 1.1 \times 10^{-3}$
8.3×10^{-4}	8.3×10^{-4}	5.0×10^{-1}	20.0	7.6×10^{-3}	1.1×10^{-2}		
8.3×10^{-4}	8.3×10^{-4}	1.0	20.0	6.9×10^{-3}	1.2×10^{-2}		
8.3×10^{-4}	8.3×10^{-4}	1.5	20.0	6.2×10^{-3}	1.0×10^{-2}		
8.3×10^{-4}	8.3×10^{-4}	1.5×10^{-1}	50.0	3.9×10^{-2}	4.7×10^{-2}	$3.2 \times 10^{-2} \pm 5.2 \times 10^{-3}$	$9.0 \times 10^{-2} \pm 2.9 \times 10^{-2}$
8.3×10^{-4}	8.3×10^{-4}	5.0×10^{-1}	50.0	3.4×10^{-2}	1.0×10^{-1}		
8.3×10^{-4}	8.3×10^{-4}	1.0	50.0	2.8×10^{-2}	1.1×10^{-1}		
8.3×10^{-4}	8.3×10^{-4}	1.5	50.0	2.8×10^{-2}	1.1×10^{-1}		

	$k^{obs}_{vinylene}$		$k^{obs}_{vinylidene}$
$\Delta H^{\ddagger}$	9.7 ± 1.2 kcal/mol	$\Delta H^{\ddagger}$	16.2 ± 3 kcal/mol
$\Delta S^{\ddagger}$	−35.0 ± 4 cal/(mol K)	$\Delta S^{\ddagger}$	−12.6 ± 6 cal/(mol K)
k(298)	9.68×10^{-3} M^{-1} s^{-1}	k(298)	1.32×10^{-3} s^{-1}

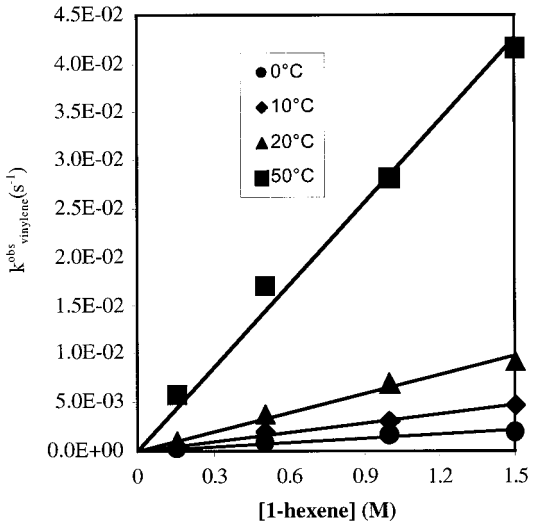

Figure 9. Plot of $k^{obs}_{vinylene}$ vs [1-hexene] for the formation of vinylene end groups (toluene, $[\mathbf{1}]_0 = 8.3 \times 10^{-4}$ M, points represent experimental data and solid lines are the results of linear regression analysis).

by correlation peaks in the ^{13}C INADEQUATE spectrum. Cross-peaks arising from 2,1 regioerrors appear in end groups only; *there is no evidence of enchained 2,1 regioerrors.* A critical observation is the absence of INADEQUATE peaks corresponding to pairs of aliphatic C atoms that would result from enchainment of a 2,1 regioerror. In contrast, several INADEQUATE peaks are found for vinylic−allylic C pairs and for allylic−aliphatic C pairs that result from termination after a 2,1 insertion. These pairs also exhibit clear $^{13}C-^{13}C$ coupling in the 1-D ^{13}C NMR spectrum (Figure 11). From these data we estimate that >95% of all 2,1 insertions result in terminations.

Under the conditions of the polymerization with labeled 1-hexene, the vinylene:vinylidene ratio is 3:1. All of the vinylidene resonances are ^{13}C labeled at the terminal position, as shown by splitting of the vinylidene ^1H NMR resonances.

The ^{13}C NMR data allow us to determine the stereo- and regiochemistry of termination following a 2,1 insertion. Ap-

Table 3. Assignment of End Groups Detected in Poly-1-hexene Formed from 99% ^{13}C-1 Labeled 1-Hexene

Peak	^{13}C δ (ppm)	End Group
A	19.69 $J_{C\text{-}D}$=18.9 Hz	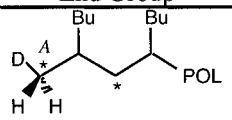
B *E*	24.27 33.92 $J_{C\text{-}C}$=34.1 Hz	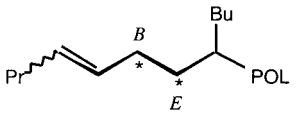
C *H*	31.44 128.25 $J_{C\text{-}C}$=43.0 Hz	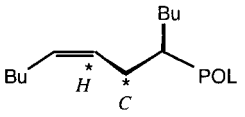
D	33.80	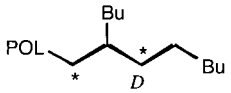
F *I*	36.67 128.40 $J_{C\text{-}C}$=43.7 Hz	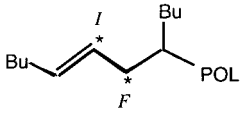
G	110.35	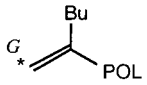

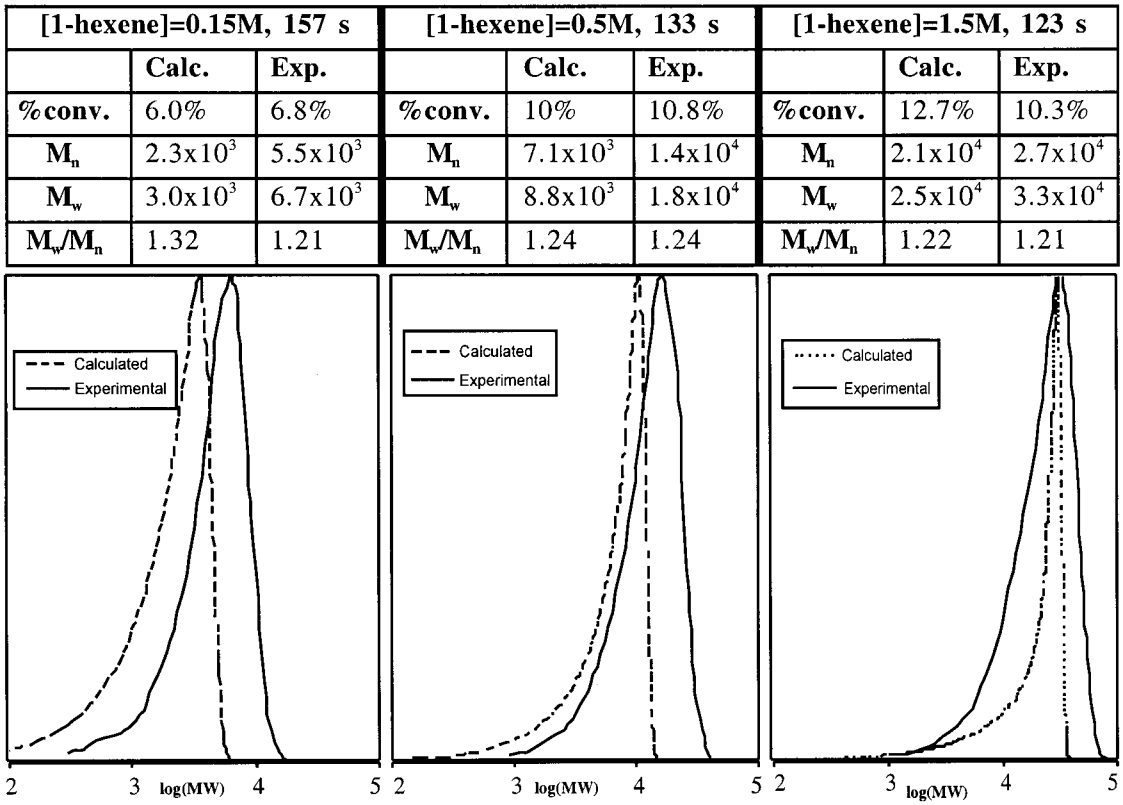

Figure 10. Experimental (GPC) and calculated poly-1-hexene molecular weight profiles obtained at the indicated initial concentration of 1-hexene and reaction time (toluene, 0 °C, $[\mathbf{1}]_0 = 6.0 \times 10^{-4}$ M).

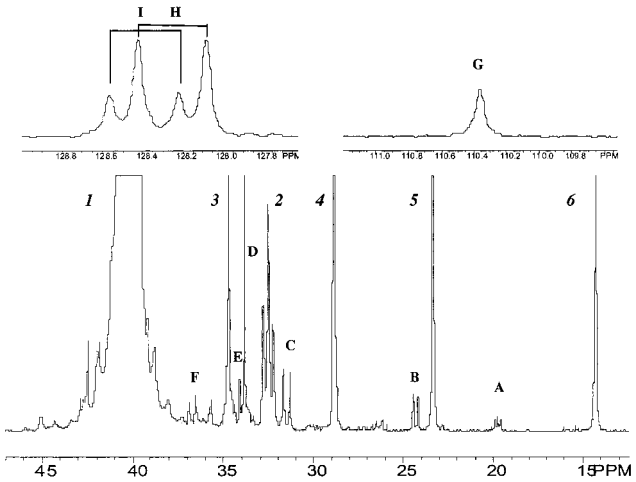

Figure 11. ^{13}C NMR (125 MHz) spectrum of poly-1-hexene obtained from the polymerization of 99% ^{13}C-labeled 1-hexene. The numbers correspond to the standard numbering of 1-hexene; C-1 is ^{13}C-enriched, whereas C-2 through C-6 are at natural abundance. Letters mark polymer microstructures described in Table 3.

Scheme 5

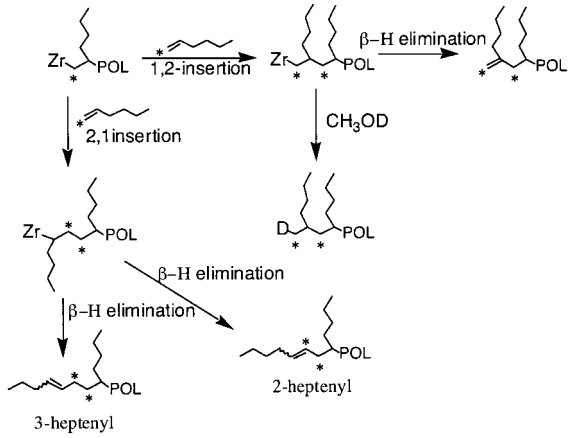

proximately 80% of these terminations involve loss of H from C-1 of the last monomer to generate a 2-heptenyl end group. Of these terminations, 70% yield *cis*-alkene and 30% yield *trans*-alkene. The 2-heptenyl end groups are readily identified in the ^{1}H NMR of the labeled polymer because one of the vinylene resonances is split by coupling to ^{13}C. The 3-heptenyl groups, which arise from loss of H at C-3 following a 2,1 insertion, constitute 20% of the vinylene end groups; the stereochemistry of these groups could not be determined conclusively from the data at hand.

Also notable in the ^{13}C NMR of labeled poly-1-hexene are resonances due to hexyl end groups and a D-labeled methyl group. The former group is the result of chain re-initiation after a β-H elimination, and the latter is due to MeOD quench of active sites. The intensities of these resonances are consistent with the vast majority of the catalyst existing as an actively propagating, primary Zr−alkyl complex. Scheme 5 provides an overview of the origins of different end groups.

Discussion

The results provided in the previous section are consistent with a catalytic process in which >90% of the catalyst exists as an actively propagating primary Zr−alkyl. No catalyst deactivation or pooling into "dormant" forms is indicated either by the active site counts or by changes in catalyst activity. A plausible, minimal mechanism for the principal initiation, propagation, and termination steps is provided in Figure 12.

Scheme 6

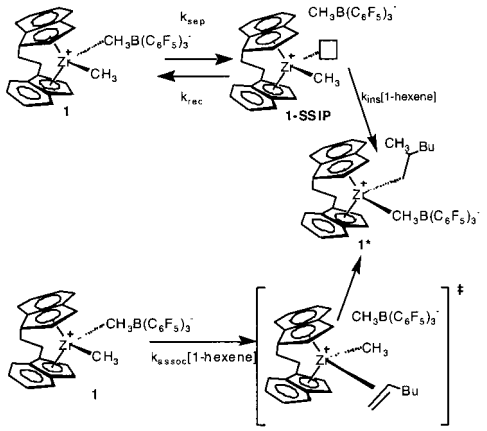

Kinetics of Initiation. Initiation follows a simple rate law: first order in [**1**] and [1-hexene] (from [1-hexene] = 0.15−1.5 M). The first-order dependence on [**1**] suggests that insertion is not promoted (or inhibited) by aggregation of **1** under the conditions studied, and the large negative entropy of activation is consistent with a simple bimolecular process. The independence of the rate on excess $B(C_6F_5)_3$ or added $[PhNMe_3][MeB(C_6F_5)_3]$ implies a simple mechanism. Two limiting mechanisms that are consistent with the observed rate law are shown in Scheme 6. In the first mechanism, conversion of a contact ion-pair (**1**) into a solvent-separated ion-pair (**1-SSIP**) precedes reaction with 1-hexene. The second mechanism corresponds to a purely associative transition state. Distinction between the two mechanisms is difficult. In the limit of a rapid pre-equilibrium between **1** and **1-SSIP**, both mechanisms predict rate laws that are first order in [1-hexene], in accord with our experimental data. Increased solvent polarity should increase the rate of either pathway because both mechanisms involve significant ion-pair separation in the transition state. A potentially distinguishing feature of the upper mechanism from Scheme 6 is a fundamental limitation on the frequency of formation of **1*** from **1**: this can be no faster than the frequency of ion-pair separation (k_{sep}). Recently we have used dynamic NMR data to estimate upper limits on the rate constant for the separation of **1** into ion-pairs.[23] The measurement involves transfer of magnetization between diastereotopic indenyl protons along a pathway that Marks has denoted as ion-pair symmetrization.[1b,17] With the assumption that ca. 50% of all ion-pair separation events yield symmetrization, $k_{sep} \approx 2k_{symm}$. We note that this is a conservative upper limit on k_{sep} because dynamic NMR studies of **1** reveal *no* evidence for any chemical exchange via a unimolecular ion-pair symmetrization process.

From the initiation rate law, the frequency with which **1** undergoes initiation is k_i [1-hexene]. Experimentally we have validated this rate law through 1-hexene concentrations as high as 1.5 M. Therefore, the product k_i [1-hexene] at [1-hexene] = l.5 M is a cautious *lower* limit estimate of the maximum initiation frequency. In Table 4 we compare the estimated *upper* limits for the frequency of ion-pair separation with estimated lower limits for the maximum frequencies of initiation at various temperatures.

(22) For analyses of poly-1-hexene by ^{13}C NMR, see: (a) Asakura, T.; Demura, M.; Nishiyama, Y. *Macromolecules* **1991**, *24*, 2334−2340. (b) Babu, G. N.; Newmark, R. A.; Chien, J. C. W. *Macromolecules* **1994**, *27*, 3383−3388.

(23) Landis, C. R; Somsook, E. *J. Am. Chem. Soc.*, submitted for publication.

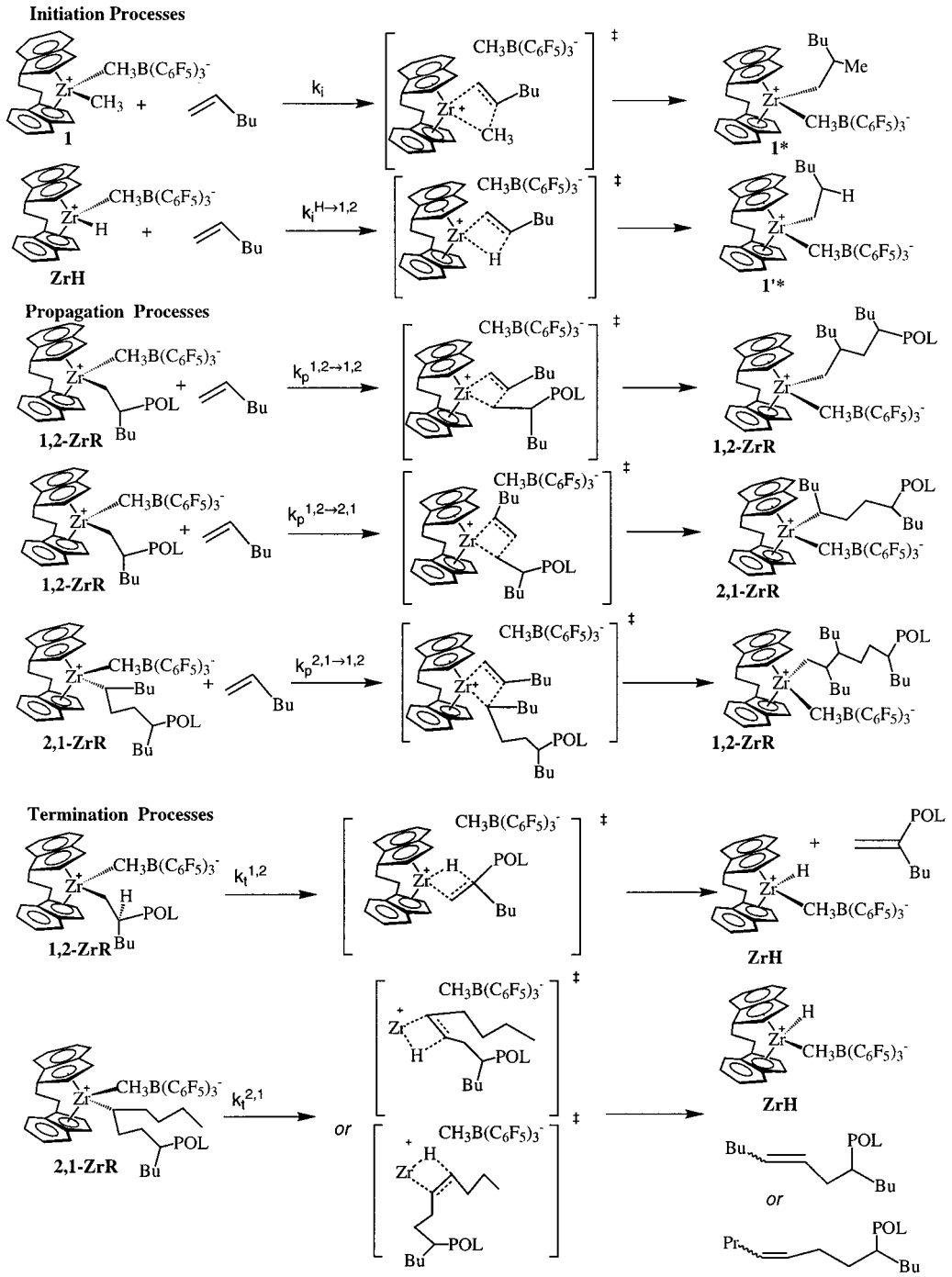

Figure 12. A plausible mechanism for the principal initiation, propagation, and termination steps in 1-hexene polymerization as catalyzed by **1**.

Table 4. Comparisons of Estimated Frequencies with Which **1** Undergoes Ion-Pair Separation (k_{sep}, s^{-1}, Upper Limit) with Observed Frequencies of Initiation (k_i [1-Hexene], s^{-1}) at 1.5 M 1-Hexene

	0 °C	10°C	20°C
k_i[1-hexene]	0.05	0.11	0.25
k_{sep}	<0.02	<0.04	<0.06

We prefer the associative mechanism for initiation of **1** as shown in Scheme 6. Although the estimations in Table 4 do not distinguish conclusively between the two mechanisms, we emphasize that these estimates are very conservative. Further support for this preference is provided by a comparison of activation enthalpies for initiation with other dynamic processes that conform to a unimolecular ion-pair symmetrization mechanism. Simple, non-*ansa*-metallocene analogues of **1** (e.g., $[(Me_4Cp)_2ZrMe]$ $[MeB(C_6F_5)_3]$ and $[(1,2\text{-}CpMe_2)_2ZrMe]$ $[MeB(C_6F_5)_3]$) undergo exchange by unimolecular ion-pair symmetrization pathways with activation enthalpies >20 kcal/mol, whereas the observed activation enthalpy for initiation of **1** is far smaller, at 11.5 ± 1.5 kcal/mol.

In a beautiful set of experiments involving the reaction of metallocene−(μ-conjugated diene)−borate betaines with simple alkenes, Erker and co-workers have measured the kinetics of the first alkene insertion.[24] Importantly, their work establishes that magnetization transfer between diastereotopic allyl resonance is *increased* by the presence of alkene via an associative process. This observation resembles the associative process that we suggest for initiation at **1**. After association of the alkene, Erker and co-workers[24b,d] propose formation of Zr(σ-allyl)-

(alkene) complexes which can either dissociate alkene or irreversibly insert. Depending on the nature of the metallocene, the ratio of dissociation to insertion varies from 3:1 to 80:1. Unlike **1**, the betaines observed by Erker undergo initiation much faster than subsequent propagation steps, presumably because the first insertion yields a particularly stable chelate in the case of the betaines.

Kinetics of Propagation. Knowledge of the concentration and nature of the propagating species simplifies analysis of the polymerization kinetics. For the polymerization of 1-hexene as catalyzed by **1** in toluene solution, we find (1) a simple rate law which is strictly first order in [1-hexene] and (2) unaffected by the addition of excess borane or $[PhNMe_3]$ $[MeB(C_6F_5)_3]$, (3) virtually all of the added catalyst is active and exists as a primary alkyl resulting from 1,2 insertions, and (4) no evidence for catalyst deactivation. Based on our previous discussion of initiation, we propose that the propagation step involves association of 1-hexene with partial displacement of the $MeB(C_6F_5)_3$ anion. This picture is supported by recent computational studies.[25] The propagation activation enthalpy is low (ca. 7 kcal/mol) and the activation entropy is large and negative, consistent with a bimolecular transition state. As with our proposed mechanism of initiation, this analysis is not conclusive nor necessarily general. The nature of the alkene, the strength of the cation−anion pairing, the solvent dielectric, and the temperature all may significantly change the nature of the propagation step.

Kinetics of Termination. Polymer molecular weights and their distribution play a critical role in determining polymer properties. If we ignore initiation effects, which is appropriate for most bulk catalytic polymerizations, the average molecular weight of polymer produced by a single-site catalyst is provided by the ratio of the sum of all propagation rates divided by the sum of all termination rates. A rational understanding of the control of molecular weights requires knowledge of termination mechanisms and rate laws.

We have determined empirical rate laws for the two major termination processes observed under our polymerization conditions: termination after a 1,2 insertion to produce a vinylidene end group and termination after a 2,1 insertion to produce vinylene end groups. The two termination processes have dramatically different rate laws. The rate of vinylidene formation is zero order in 1-hexene, whereas the vinylene rates are first order in 1-hexene. From a phenomenological viewpoint, different rate laws are not surprising because there is evidence from the polypropene literature that the vinylene/vinylidene ratio depends on [propene].[6a,b,13a,b] Because we have established that the steady-state distribution of catalyst species consists almost entirely of primary alkyls resulting from 1,2 insertions, we can now interpret the empirical rate laws for termination in terms of elementary processes.

The simplest mechanism for formation of vinylidene end groups is unimolecular β-hydride elimination following a 1,2 insertion. The activation parameters that we observe for this process ($\Delta H^{\ddagger} = 16.2 \pm 3$ kcal/mol, $\Delta S^{\ddagger} = -12 \pm 6$ cal/(mol K)) and the net rates are reasonably consistent with previous measurements of unimolecular β-hydride elimination rates.[26]

Scheme 7

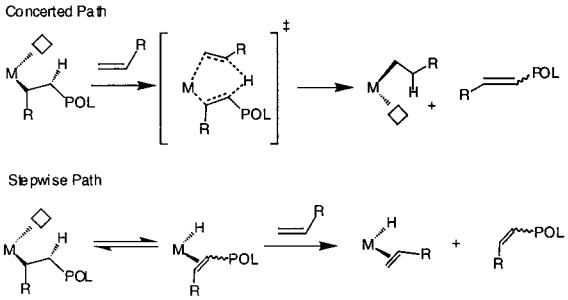

Characterization of ^{13}C-labeled polymer clearly indicates that vinylene end groups are formed after 2,1 insertion with a rate that is first order in 1-hexene. To the best of our knowledge, the only mechanistic interpretation of termination rate laws that are first order in monomer concentration has been bimolecular chain transfer to monomer.[13a] Scheme 7 illustrates two plausible mechanisms[7,27] for bimolecular chain transfer to monomer: concerted β-H transfer and stepwise β-H elimination with associative displacement of the coordinated alkene. Interpreting our results in terms of a bimolecular chain transfer mechanism creates a conundrum: Why should the bulkier secondary alkyl exclusively terminate by a bimolecular mechanism whereas less bulky primary alkyls terminate unimolecularly?

The rate laws of catalytic processes reflect the steady-state distribution of catalyst species. For the polymerization of 1-hexene as catalyzed by **1**, primary alkyls resulting from 1,2 insertion dominate the catalytic speciation, and 2,1 insertions are infrequent. Furthermore, ^{13}C NMR spectra of labeled 1-hexene demonstrate that insertion of another monomer after a 2,1 insertion, which would create an enchained regioerror, is much less likely than termination. Taken together, *these observations suggest a kinetic scenario (see Figure 12) in which the mechanism of both termination processes is simple β-hydride elimination but the vinylene end group appears with a rate that is proportional to [1-hexene].*

In Figure 12, ZrH represents hydride formed from β-H elimination, 1,2-ZrR represents all primary alkyls formed from 1,2 insertion, and 2,1-ZrR represents all secondary alkyls formed by 2,1 insertion. Note that the rate constants for the elementary steps in Figure 12 differ from the rate constants for the phenomenological steps in the Results section. Figure 12 contains several assumptions that simplify the analysis but are not critical to the conclusions: the stereochemistries of intermediates 1,2-ZrR and 2,1-ZrR are ignored, and reaction of ZrH with alkene to produce a secondary alkyl (2,1-Zr) is negligible, as are sequential 2,1 insertions. Application of standard steady-state approximations leads to steady-state concentrations of 1,2-ZrR and 2,1-ZrR following catalyst initiation as shown below:

$$[\text{1,2-ZrR}] \approx \frac{k_p^{2,1\rightarrow 1,2}\,[\text{2,1-ZrR}]\,[\text{alkene}] + k_i^{H\rightarrow 1,2}\,[\text{alkene}]\,[\text{ZrH}]}{k_p^{1,2\rightarrow 2,1}\,[\text{alkene}] + k_t^{1,2}}$$

$$[\text{2,1-ZrR}] \approx \frac{k_p^{1,2\rightarrow 2,1}\,[\text{1,2-ZrR}]\,[\text{alkene}]}{k_p^{2,1\rightarrow 1,2}\,[\text{alkene}] + k_t^{2,1}}$$

Our data clearly demonstrate that the vast majority of the catalyst exists as 1,2-Zr. On the basis of this observation, we can

(24) (a) Erker, G. *Acc. Chem. Res.* **2001**, *34*, 309−317. (b) Karl, J.; Dahlmann, M.; Erker, G. *J. Am. Chem. Soc.* **1998**, *120*, 5643−5652. (c) Dahlmann, M.; Erker, G.; Nissinen, M.; Frölich, R. *J. Am. Chem. Soc.* **1999**, *121*, 2820−2828. (d) Dahlmann, M.; Erker, G.; Bergander, K. *J. Am. Chem. Soc.* **2000**, *122*, 7986−7998.

(25) (a) Chan, M. S. W.; Ziegler, T. *Organometallics* **2000**, *19*, 5182−5189. (b) Lanza, G.; Fragalà, I. L.; Marks, T. J. *J. Am. Chem. Soc.* **1998**, *120*, 8257−8258. (c) Lanza, G.; Fragalà, I. L.; Marks, T. J. *J. Am. Chem. Soc.* **2000**, *122*, 12764−12777.

(26) (a) Guo, Z.; Swenson, D. C.; Jordan, R. F. *Organometallics* **1994**, *13*, 1424−1432. (b) Alelyunas, Y. W.; Guo, Z.; LaPointe, R. E.; Jordan, R. F. *Organometallics* **1993**, *12*, 544−553.

approximate the steady-state concentration of 1,2-Zr as equal to the total concentration of all Zr-containing species, Zr^{TOT}.

$$[Zr^{TOT}] = [1,2\text{-ZrR}]$$

Hence, the rates of vinylidene and vinylene end group formation are given by eqs 9 and 10.

$$\frac{\partial[\text{vinylidene}]}{\partial t} = k_t^{1,2}\,[Zr^{TOT}] \tag{9}$$

$$\frac{\partial[\text{vinylene}]}{\partial t} = k_t^{2,1}\left[\frac{k_p^{1,2\rightarrow 2,1}\,[Zr^{TOT}]\,[\text{alkene}]}{k_p^{2,1\rightarrow 1,2}\,[\text{alkene}] + k_t^{2,1}}\right] \tag{10}$$

Clearly, vinylidene end group formation will be independent of [alkene]. However, in the limit of fast termination relative to alkene insertion for 2,1-ZrR, the rate of vinylene end group formation simplifies to a process that is first order in [alkene] (eq 11).

$$\text{if} \quad k_t^{2,1} \gg k_p^{2,1\rightarrow 1,2}\,[\text{alkene}]$$

$$\frac{\partial[\text{vinylene}]}{\partial t} = k_p^{1,2\rightarrow 2,1}\,[Zr^{TOT}]\,[\text{alkene}] \tag{11}$$

Taking into consideration experimental uncertainties and the range of alkene concentrations used, the data require that $k_t^{2,1}$ is at least 6-fold greater than the quantity $k_p^{1,2\rightarrow 2,1}\,[Zr^{TOT}]$.

Put simply, the kinetic scenario outlined above dictates that each 2,1 insertion commits the chain to termination. Under these conditions, the rate at which vinylene end groups appear is given by the rate of misinsertion. The critical test of this scenario is an absence of enchained regioerrors. Analysis of the microstructure of ^{13}C-labeled poly-1-hexene demonstrates that this requirement is satisfied. If one accepts this interpretation of the termination kinetics, then *the rate constants and apparent activation parameters (see Table 2) measured for termination to a vinylene end group correspond to the kinetic parameters for 2,1 insertion of 1-hexene at* ***1*****. As such, the activation enthalpy for 2,1 insertion (9.7 kcal/mol) is approximately 3.3 kcal/mol higher than that for 1,2 insertion (6.4 kcal/mol). The failure of secondary alkyls resulting from 2,1 insertion to accumulate combined with the absence of enchained regioerrors suggests that secondary alkyls undergo β-hydride elimination much faster than primary alkyls. Thus, there is no support for the contention that secondary alkyls will accumulate because they are slow to insert or β-hydride eliminate.

We emphasize that *our data do not exclude a bimolecular termination process* for the formation of vinylene end groups. If termination from 2,1-Zr were exclusively bimolecular, the rate of vinylene formation would be strictly first order in [alkene] over all conditions. Such a scenario would not place any limits, high or low, on the ratio of 2,1 enchainments to terminations. Kinetically, the distinguishing feature between the bimolecular and unimolecular 2,1-Zr termination processes is that the former requires a fixed ratio of enchainments to terminations as [1-hexene] is increased, whereas the latter requires that the ratio increase. Our data cannot conclusively distinguish between these mechanisms because we see no evidence of enchained regioerrors even at high concentration of 1-hexene.

Summary

The recent history of metallocene-catalyzed alkene polymerization reactions demonstrates that apparently minor changes in catalyst structure, the nature of the activator, solvent polarity, and the alkene can lead to surprising changes in catalyst activity, chemo-, regio-, and stereoselectivity, and termination products. Caution, therefore, is required in extrapolating the results presented herein to any other systems. Mindful of these caveats, we now compare the main conclusions of our work with existing data for related systems. We begin with a comparison of MAO vs $B(C_6F_5)_3$ activators and conclude with a comparison of 1-hexene and propene polymerization.

We distinguish between catalyst activation and initiation: activation is the process of generating the catalyst ion-pair **1** from the catalyst precursors, whereas initiation refers to the first insertion of alkene into the Zr−Me bond of **1**. The first insertion of 1-hexene into a Zr−Me bond is significantly slower than subsequent insertions of 1-hexene into the growing polymer chain. At 0 °C, the ratio k_p/k_i equals 70, a ratio that is fortuitously close to values (ca. 120) estimated by Herfert and Fink[6c] from studies of ethene polymerization catalyzed by $Cp_2TiCl_2-AlRCl_2$ systems under very different conditions. Increased temperatures decrease the k_p/k_i ratio due to the lower activation enthalpy of propagation relative to initiation. Two factors may contribute to the slow rate of initiation relative to propagation: (1) the greater strength of the Zr−Me bond relative to the $Zr-CH_2-POL$ bond and (2) weakened ion-pairing in the propagating species resulting from its larger steric bulk. Relevant to the latter point, Marks and Beswick[28] have found that symmetrization of $[(Me_2Cp)_2Zr(R)]\,[MeB(C_6F_5)_3]$ complexes via an ion-pair symmetrization pathway increases as the steric bulk of R increases.

As noted by Herfert and Fink,[6c] the relative slowness of insertion into M−Me bonds complicates analysis of propagation kinetics in the presence of any chain transfer agent (such as MAO) which is capable of exchanging a Me group back on the active catalyst. As a rough guideline, under conditions where such chain transfer limits molecular weights to ca. <300 monomer units, a significant fraction of the catalyst will accumulate in the form of uninitiated M−Me species. Because the D-labeling strategy we have used permits direct measurement of initiation rates and rate laws, and because **1** behaves as a truly single-site polymerization catalyst, we have been able to rigorously analyze the propagation kinetics without complications due to catalyst methylation by chain transfer to Al.

Previous studies on 1-hexene polymerization by Deffieux and co-workers[10a] using *rac*-$(C_2H_4(1\text{-indenyl})_2)ZrCl_2$ and MAO as activator led to conclusions similar to ours: the rate of propagation is first order in [1-hexene], and the catalyst is long-lived. The propagation rates increase with increased concentration of MAO, but the effect levels off at [MAO]:[Zr] > 3000. If one assumes that the active site concentration is equal to $[Zr]^{TOT}$, then the data of Deffieux and co-workers[10a] lead to a propagation rate constant of ca. 60 $M^{-1}\,s^{-1}$ in toluene at 20 °C. Comparison with the value of 6.3 $M^{-1}\,s^{-1}$ that we have determined for $B(C_6F_5)_3$ activation makes it appear that propagation for the MAO-activated catalyst is 10 times greater than that of the $B(C_6F_3)_3$-activated catalyst at 20 °C.

(27) (a) Woo, T. K.; Fan, L.; Ziegler, T. *Organometallics* **1994**, *13*, 2252−2261. (b) Cavallo, L.; Guerra, G. *Macromolecules* **1996**, *29*, 2729-2737. (c) Lohrenz, J. C. W.; Woo, T. K.; Ziegler, T. *J. Am. Chem. Soc.* **1995**, *117*, 12793−12800. (d) Moscardi, G.; Resconi, L.; Cavallo, L. *Organometallics* **2001**, *20*, 1918−1931.

(28) (a) Beswick, C. L.; Marks, T. J. *Organometallics* **1999**, *18*, 2410−2412. (b) Beswick, C. L.; Marks, T. J. *J. Am. Chem. Soc.* **2000**, *122*, 10358−10370.

Polymerization of 1-hexene with **1** is a highly regioselective and stereoselective process. Analysis of the poly-1-hexene microstructure reveals isotacticities that exceed 99% *mmmm* pentads and a complete lack of enchained regioerrors. At 20 °C, 1,2 insertions are 900 times[29] more likely than 2,1 insertions. Chain termination is dominated by β-hydride elimination, yielding two classes of unsaturated end groups, vinylene and vinylidene.

Interestingly, Deffieux and co-workers[10d] reported molecular weights and isotacticities for poly-1-hexene obtained with MAO as the activator that are similar to those found in this work, but they found that the molecular weights are independent of [1-hexene]. For MAO-activated polymerization of 1-hexene with catalytic *rac*-((dimethylsilyl)bis(4,5,6,7-tetrahydro-1-indenyl))-$ZrCl_2$, Odian et al.[10c] report that increasing temperature favors termination to yield vinylidenes relative to vinylenes, similar to our results. We propose that chain termination for the MAO-activated reaction is dominated by a second-order process: first order in [Zr] and first order in [1-hexene], and predict primarily vinylene end groups. Indeed, preliminary results with MAO and borate activators are consistent with this prediction. Because both propagation and termination rates are first order in [1-hexene], the overall molecular weights are independent of [1-hexene]. Based on the results of Deffieux[10d] and our own preliminary results with a variety of activators, we characterize $B(C_6F_5)_3$ activator as yielding tighter ion-pairs, slower propagation rates, and a higher ratio of unimolecular/bimolecular termination rates relative to MAO and borate activators.

From literature reports it is clear that propene polymerizations exhibit more complex kinetic behavior than we find for 1-hexene polymerization.[2a,6,13] Among the more complex behaviors are (1) propagation rate laws that approach[6] second order in [propene], (2) large changes in catalyst activity through a kinetic run, (3) lower stereospecificity due to epimerization, (4) a greater variety of end groups, and (5) a greater degree of enchained regioerrors, including 3,1 enchainments. Many of these features change significantly with rather subtle alteration of the catalyst structure.

As Resconi et al. succinctly summarize, catalyst deactivation during propene polymerization "makes it difficult to determine the precise number of active centers and hampers a correct kinetic analysis".[2a] In principle, the combination of active site counting and kinetic methods that we have employed for the study of 1-hexene polymerization applies to propene polymerization as well. In particular, the putative role of relatively inactive M−allyl complexes should be directly addressable by the NMR of quench-labeled polymers. We are actively pursuing this line of research.

Some features of chain termination are common between propene and 1-hexene polymerizations. For example, Resconi and co-workers[13] indicate that the kinetics of vinylene end group formation depends on [propene], whereas vinylidene end group formation appears to be independent of [propene]. For propene polymerization with *rac*-$(C_2H_4(1\text{-indenyl})_2)ZrCl_2$/MAO, the vinylene resonances are primarily cis, as we have found for 1-hexene.

The kinetic scenario for termination that we propose models the observed degrees of polymerization (P_n) as a function of monomer concentration for propene polymerization. If we assume that most of the active catalyst is the primary alkyl, [1,2-ZrR], and that this species carries all of the propagation flux, then the following expression for the degree of polymerization pertains:

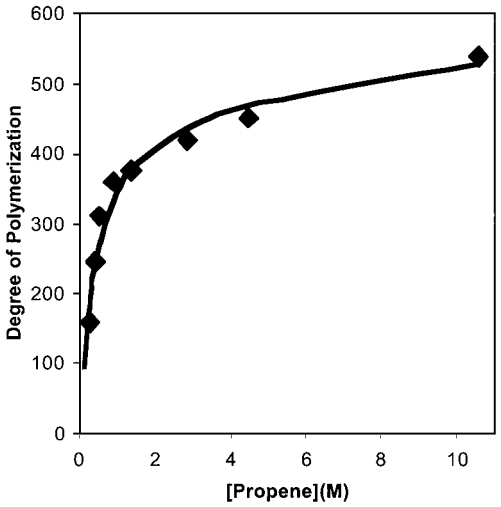

Figure 13. Computed (solid line) and observed (points) data for the degree of polymerization (P_n) of propene as catalyzed by *rac*-$(C_2H_4(1\text{-indenyl})_2ZrCl_2$/MAO in toluene solution at 59 °C (experimental data taken from ref 13a).

$$P_n \approx \frac{R_p}{R_t} \approx \frac{k_p^{1,2\rightarrow1,2}\,[\text{alkene}]}{k_t^{1,2} + \dfrac{k_t^{2,1}k_p^{1,2\rightarrow2,1}\,[\text{alkene}]}{k_p^{2,1\rightarrow1,2}\,[\text{alkene}] + k_t^{2,1}}} \qquad (12)$$

This expression can be simplified to three terms (*A*, *B*, *C*) by taking appropriate ratios of the five individual rate constants:

$$P_n \approx \frac{R^{\text{prop}}}{R^{\text{term}}} \approx \frac{A\,[\text{alkene}]}{1 + \dfrac{B\,[\text{alkene}]}{C\,[\text{alkene}] + 1}}$$

$$\left(A = \frac{k_p^{1,2\rightarrow1,2}}{k_t^{1,2}},\quad B = \frac{k_p^{1,2\rightarrow2,1}}{k_t^{1,2}},\quad C = \frac{k_p^{2,1\rightarrow1,2}}{k_t^{2,1}}\right) \qquad (13)$$

As shown in Figure 13, this expression fits the published experimental data quite well ($A = 1300$, $B = 2.8$, $C = 0.02$). However, a more detailed analysis reveals that this model underestimates the observed number of enchained regioerrors: in liquid propene (10.4 M) the value of $C = 0.02$ leads to a 5:1 ratio of vinylenes/enchained regioerrors. The data reported by Resconi[13a] indicate a 1:5 ratio.

It has been observed that that the ratio of 2,1 enchainments/1,3 enchainments for polymerization of propene by C_2-symmetric *ansa*-metallocenes varies linearly with propene concentration.[13a,d] Busico[13d] and Resconi[13a] have interpreted this ratio to indicate that insertion of propene following a 2,1 insertion is bimolecular (first order in monomer), whereas isomerization is unimolecular. This is consistent with our overall mechanism. However, data for the less regioselective catalyst *rac*-$(C_2H_4\text{-}(4,7\text{-}Me_2\text{-}1\text{-indenyl})_2)ZrCl_2$/MAO reveal that monomer concentration affects the partitioning between *termination* and 3,1 isomerization following a 2,1 insertion: the ratio of *cis*-2-butenyl/3,1 enchainments is first order in monomer. This result is not consistent with our mechanism, which predicts that the ratio is monomer independent. Resconi has argued that the monomer concentration dependence is evidence for a bimolecular chain transfer to monomer termination step.[13a]

At this point, the mechanistic aspects of fundamental steps in alkene polymerization, particularly chain termination and the

(29) This factor is determined from measurements at 20 °C; a factor of 790 is calculated from the activation parameters.

origin of complex dependencies of propagation rates on monomer concentration, are poorly understood and seem to vary considerably with catalyst, monomer, and activator. Resolution of these and other issues will require more detailed data on the speciation of the catalyst as a function of the reaction conditions, which again underscores the value of active site counting methods.

In summary, we demonstrate what we believe is the first simultaneous determination of time-dependent active site counts and initiation, propagation, and termination rate laws for a well-defined metallocene-catalyzed polymerization of a terminal alkene. The initial insertion of 1-hexene into a Zr−Me bond is ca. 70-fold slower than all subsequent insertions. Propagation and initiation are strictly first order in [1-hexene]. On the basis of comparison of initiation rates with NMR-derived chemical exchange rates, we tentatively conclude that ion-pair separation need not precede insertion into the Zr−Me bond. Two termination processes are observed: a first-order process that produces vinylidene end groups and a second-order process that produces vinylene end groups. Steady-state kinetic analysis reveals that termination to form vinylene end groups, which is first order in monomer, does not require bimolecular chain transfer to monomer as is commonly assumed. A process in which each regioerror is committed to terminate chain growth accounts for both the rate law and the observation of no enchained regioerrors. This interpretation emphasizes the dramatic influence of regioselectivity on polymer molecular weights. The methods and results described herein form a solid base for further exploration of the mechanisms of metallocene-catalyzed polymerization reactions, which are currently underway.

Acknowledgment. We thank the Department of Energy, Office of Basic Energy Sciences, and Dow Chemical Co. for support of this work. NMR facilities used in this research were supported by grants NSF CHE-9629688, NSF CHE-8813550, NIH 1S10 RR04981-01, NSF CHE-9208463, and NIH 1 S10 RR0 8389-01. We thank Mr. Doug Sillars for his valuable comments on this manuscript. The helpful suggestions of Prof. Hans-Herbert Brintzinger and Mr. Frank Schaper are acknowledged with gratitude.

JA016072N